Order Number 9218228

Interactive multidimensional NMR spectrum simulation

Chen, Wenqiao, Ph.D.

City University of New York, 1992

U·M·I
300 N. Zeeb Rd.
Ann Arbor, MI 48106

INTERACTIVE MULTIDIMENSIONAL NMR SPECTRUM SIMULATION

WENQIAO CHEN

A dissertation submitted to the Graduate Faculty in Chemistry in partial fulfillment of the requirements for the degree of Doctor of Philosophy, The City University of New York.

1992

This manuscript has been read and accepted for the Graduate Faculty in Chemistry in satisfaction of the dissertation requirement for the degree of Doctor of Philosophy.

1/30/92 — L M Massa

Date — Chair of Examining Committee

1/31/92 — Richard Pinn

Date — Executive Officer

Professor M. Diem

Professor L. Massa

Professor S. Greenbaum

Professor R. Stark

Professor W. Sweeney

Supervisory Committee

The City University Of New York

Abstract

INTERACTIVE MULTIDIMENTIONAL NMR SPECTRUM SIMULATION

by

Wenqiao Chen

Adviser: Professor Lou Massa

A new algorithm for nmr spectrum simulation has been developed. It is based on the fact that when the Hamiltonian operator of the spin system is represented in a special form of matrix by the direct product method, the Hamiltonian matrix can be diagonalized easily, and the eigenvalues and eigenvectors can be obtained efficiently through a group of recursive formulae. Preliminary results show that the new algorithm, when

implemented on a microvax/vms machine, is able to simulate spectra of larger spin coupling networks (up to 16 spins) than can be done by currently available programs, such as LAOCN5. Further, since the Single Spin Single Quantum Transitions (SSSQT) carry a major portion of the structural information, and represent the majority of the total observable coherences, the simulation process can therefore be speeded up substantially, if SSSQT are taken as an approximation of the whole spectrum. This approximation makes a real time response to modifications of chemical shift and J coupling parameters for coupling networks of many more than 5~6 spins (I=1/2) possible, allowing direct interactive comparison of experimental and simulated spectra.

Finally, a 3D spectrum simulation program is developed and implemented on an Evans & Sutherland PS-390 graphics station. Its application for interactive spectrum assignment and for the conformational investigation of biological macromolecules is discussed.

Acknowledgements

This work was supported, in part, by awards from the National Institutes of Health CA46713 (award to Prof. M. S. Broido) and RR03037 (Research Centers in Minority Institutions award to Hunter College). Here, I express my appreciation to Prof. Broido for her advice and support in the first period of this work.

I should like to express my appreciation to Dr. M. Diem, Dr. S. Greenbaum, Dr. R. Stark, Dr. G. Quigley, Dr. M. Mezei, Dr. W. Sweeney, and Dr. M. Blumenstein for their great help and encouragement. Especially I must express my appreciation to Prof. L. Massa, who, with his great help at a critical moment, made it possible for me to continue this work and finish this project.

CONTENTS

List of Illustrations

Section 1 Introduction

In the past decade, nuclear magnetic resonance spectroscopy has been extensively used as one of the most powerful tools to elucidate molecular structure, especially in the solution environment where other techniques such as X-ray diffraction cannot be used[1-3].

The entire process of solving a structural problem by nmr spectroscopy may, more or less arbitrarily, be divided into two stages. First, when the structure is entirely unknown, the spectroscopist has to use the nmr data of other known molecules, combined with information about the unknown sample from chemical or from other physical techniques such as mass or vibrational spectra, to assign the nmr spectrum, until one or several structures can be elucidated as possible candidates. This stage can be called the "from spectra to structure" approach. If there are one or more structural candidates, then the spectrum of each one of them could be calculated from the measured or estimated chemical shifts and J coupling constants, and the simulated spectra then compared with the experimental data. This can be termed the "from

structure to spectra" approach. The correspondence between a structure and a spectrum should be confirmed when both approaches lead to identical results.

In practice, however, the second stage is often omitted, not because it lacks importance, but rather, that there are two basic difficulties which make it difficult. First, the values of chemical shifts and J coupling constants for a specific candidate structure can be difficult to estimate precisely; secondly, to be practical for most applications, when a coupling network contains more than nine spins, spectral calculation is both too slow and too expensive.

Recently, several data bases of chemical shift values have been compiled[4,27], making it possible to estimate these parameters within a certain precision. Additionally, the multidimensional nmr technology, specifically 3D and 4D nmr methods, reduce the degree of spectral overlap which are obstacles to spectral interpretation. With the 3D or 4D spectrum, the assignment is usually conducted on the 2D sectional planes, where it is the total pattern of the cross peaks' appearance, rather than the exact positions or the intensities of individual peaks, which characterize the structural features such as the topology of spin coupling networks, the interresidue linkages, etc.

The combination of these two developments will make the "from structure to spectra" approach more practical, provided that a fast, powerful program is available for spectral calculation from the chemical shift and coupling constant input.

SIMPL is an interactive program designed exactly for this purpose. It is capable of calculating the 1D spectrum of large molecules including coupling networks of up to 16 spins, on a microvax-II computer with 9MB board memory (all data of the performance of the program cited in this paper were measured on this machine). It can also create an approximate 3D spectrum for peptides with known amino acid sequence, from a simple chemical shift data base. This 3D spectrum can be used to speed up the assignment of the experimental 3D spectrum, and the chemical shift data base is updated automatically if the experimental peak deviates from the range specified in the data base.

Both the 1D and 3D approximate spectra can be modified almost simultaneously as input parameters change. This allows the interfacing of SIMPL with a molecular modeling program, so a user

can continuously observe the simulated nmr spectrum while manipulating the molecular structure.[1]

---

[1] Since the exact NOE intensities must be calculated through the total relaxation network including all the spins, and the internuclear distances obtained this way contain relatively large uncertainties, no provision for calculating NOE intensities has been included in SIMPL.

Section 2 Density Matrix Formalism of the NMR Experiment[2,5]

§ 2.1 Quantum Mechanical Description of an NMR Spectrum[8-12]

An nmr spectrum, $I(\omega)$, is an intensity function of frequency. It is the Fourier transformation of a signal function of time, S(t). When S(t) is obtained by quadrature detection, it is proportional to the sample's magnetization component within the probe coil effective plane, $M^+(t)$, which is usually defined as the X-Y plan if the direction of the external magnetic field B_0 is selected as the Z direction (see appendix):

$$S(t) \propto M^+(t) = M_x(t) + iM_y(t) \qquad [2.1]$$

where $M^+(t)$, in turn, is proportional to the expectation value of the X-Y component of the total spin angular momentum F^+, at the moment of detection t:

$$M^+(t) = N\gamma h \{<F^+>(t)\} = N\gamma h \text{ tr } \{F^+\sigma(t)\} \qquad [2.2]$$

Here N is the number of spin systems per unit volume, γ is the gyromagnetic ratio of the spin in discussion, and $\sigma(t)$ is the density

operator of the spin system at the moment of t[5]. $F^+ = F_x+iF_y=\Sigma(I_x+iI_y)$ is time-independent. The time dependence of the expectation value of $<F^+>(t)$ is included in the density operator $\sigma(t)$.

The matrix representation of F^+, if expanded in the spin-product function space, contains many zeroes. Therefore, not all elements of $\sigma(t)$ have contributions to the trace in Eq.[2.2]. Since only those coherences (the off-diagonal elements of the $\sigma(t)$ matrix) that contribute to the trace $tr\{F^+\sigma(t)\}$ are observable and eventually show a peak in the final spectrum, they are termed observable coherences. The row and column states of these coherences differ by one $\hbar$ in their total spin angular momentum, hence these coherences are termed single quantum transitions (SQT). It is the time dependence of these elements which determine the frequency of each spectral line.

The behavior of the spin system at the moment t, described by the density operator $\sigma(t)$, depends on the thermal equilibrium state of the system at the beginning of the experiment, $\sigma(eq)$, and the total history of the spin system during the entire period from the beginning (t=0) to the detection moment (t=t), described by propagator U(t):

$$\sigma(t) = U(t)\ \sigma(eq)\ U^{-1}(t) \qquad [2.3]$$

The standard treatment of the propagator, U(t), can be found elsewhere[6]. Here, for the sake of simplicity, assume U(t) is describing the effect of a pulse with duration of τ and follows free precession for a period of t, without the decay of relaxation[2]. Under this assumption, U(t) can be separated into two parts, an operator $R(\tau)$ of the pulse rotation around the y axis, and an operator P(t) of the free precession around the z axis:

$$U(t) = R(\tau)\ P(t) = \exp\ (-i\gamma B_1 \tau F_y)\ \ \exp\ (-iHt), \qquad [2.4]$$

where $R(\tau) = \exp\ (-i\gamma B_1 \tau F_y) = \exp\ (-i\phi F_y)$ describes the perturbation applied on the spin system during the time of τ by an RF radiation field B_1 along the direction y; and $P(t) = \exp\ (-iHt)$ describes the precession during the time t under the Hamiltonian H. Usually the moment t can be selected in such a way that during period t, an average, time-independent Hamiltonian H of the spin system can be well defined.

Putting Eq. [2.4] into Eq. [2.3], one obtains:

---

[2] Relaxation considerations can be added later, which have no effect on the direct product formalism, but will complicate the description.

$$\sigma(t) = \exp(-iHt)\ [\ \exp(-i\varphi F_y)\ \sigma(eq)\ \exp(i\varphi F_y)\ ]\ \exp(iHt) =$$

$$= \exp(-iHt)\ \sigma(\tau)\ \exp(iHt). \qquad [2.5]$$

The inner part of Eq. [2.5], $\sigma(\tau)$, is the density operator of the system at the end of the RF pulse. The effect of the pulse is to rotate the system's magnetization, around axis y of the rotating frame, by an angle of $\varphi = \gamma B_1 \tau$. The analytical form of $\sigma(\tau)$ can be obtained either by matrix multiplication, or by abstract rotation of the operator subspaces summarized by Sorenson et al[8]. The result can be written as:

$$\sigma(t) = [1-\beta_T\omega_0(F_z\cos\varphi+F_x\sin\varphi)]\ /\ tr\{\mathbf{1}\} \qquad [2.6]$$

under the assumption that both high-temperature and high-field approximations hold, i.e.,

$$\sigma(eq) = [1-\beta_T\omega_0 F_z]/tr\{\mathbf{1}\} \qquad [2.7]$$

where $\beta_T = h/(kT)$, k is the Boltzmann constant, and ω_0 the Larmor frequency of the spin species under discussion.

Now we calculate exp(+iHt) in Eq. [2.5]. When H is diagonal, Eq. [2.5] can be expressed explicitly with the matrix elements:

$$\sigma_{ij}(t) = \sigma_{ij}(t)\ \exp(i(H_{jj}-H_{ii})t/h) = \sigma_{ij}(t)\ \exp(-i\omega_{ij}t) \qquad [2.8]$$

This form is convenient when it is used in Eq. [2.2]:

$$M^+(t) = N\gamma h\Sigma_{i>j} F^+_{ji} \sigma_{ij}(t) \exp(-i\omega_{ij}t) \qquad [2.9]$$

since the Fourier transformation of S(t) can be treated explicitly:

$$I(\omega) = N\gamma h\Sigma_{i>j} F_{ij}^+ \sigma_{ji}(t) \delta(\omega-\omega_{ij}) \qquad [2.10]$$

here the δ function is a consequence of the fact that the relaxation is completely ignored, and this kind of spectrum is refered to as a "stick spectrum". When relaxation is included,

$$I(\omega) = N\gamma h\Sigma_{i>j}F_{ij}^+ \sigma_{ji}(t) [1/(\lambda_{ij}+i(\omega-\omega_{ij})] \qquad [2.11]$$

with $\lambda_{ij}=1/(T_2)_{ij}$, the decay coefficient of the resonance $I(\omega_{ij})$.

Such an explicit form is highly desirable, because it relates the off-diagonal element of density matrix $\sigma_{ij}(t)$ with the corresponding energy difference of two eigenstates $|i\rangle$ and $|j\rangle$:

$$\omega_{ij} = (H_{jj}-H_{ii})/h. \qquad [2.12]$$

When H is not diagonal, the explicit form of Eq. [2.10] can still be obtained, providing the trace of $\{F^+\sigma(t)\}$ is calculated in the eigenspace of the Hamiltonian, instead of the spin product function space:

$$M^+(t) = N\gamma h \, tr\{F^+\sigma(t)\} = N\gamma h \, tr\{(F^+)_e \, (\sigma(t))_e\}$$

$$= N\gamma h \, tr\{(T \; F^+ \; T^{-1})(T \; \sigma(t) \; T^{-1})\} \qquad [2.13]$$

since the normal orthogonal transformation will not change the trace.

Therefore,

$$M^+(t) = N\gamma h \, tr\{[F^+]_e \, [\sigma(t)]_e\} = N\gamma h \, \Sigma_{ij}[F^+{}_{ij}]_e \, [\sigma_{ji}(t)]_e \, \exp(-i\omega_{ij}t) \qquad [2.14]$$

where the subscript e denotes the eigenspace.

§ 2.2 Practical Difficulties in Spectral Calculation

The size of the matrices H, T, F^+, and σ is $(2I+1)^N \times (2I+1)^N$, where I is the spin quantum number of the nuclear species and N is the number of spins coupled together within a network. For a network of ten protons, they are 1024×1024 matrices. Although H is block diagonal, the largest block still has a size of 252×252. When H is not diagonal, the main computing load is for the calculation of T, the eigenvector matrix.

Currently the best method available, to the knowledge of the author, is an improved version of the classic Jacobi method - the Givens method, or the Householder method[15, 16]. This method involves first converting H into a triangular form, and then eliminating the off-diagonal elements row by row. The total computing load is proportional to the third power of the matrix's size, which itself increases exponentially with N, leading to a total computing load proportional to $(2I+1)^{3N}$. After the matrix T is obtained, all the other matrices must be transformed by T, and every step of matrix multiplication means an extra load which is proportional to $(2I+1)^{4N}$. Thus these calculations are very expensive

when N is large. For this reason many simulations currently being attempted are made under the "weak coupling" assumption where the eigenvector matrix T need not be calculated. However, if the coupling is strong, T must be calculated, so some other means must be found to simplify the simulation.

It should be pointed out, however, that the precision of the calculation needs to be carefully considered, since the required precision is directly related to the condition under which the simulated spectrum will be compared with the experimental one. For a crowded 1D proton spectrum with average line width of ~1Hz and with overlap existing in many regions, the precision in the frequency domain may be set to better than 0.1 Hz. On the other hand, if a 2D section of a 3D or 4D spectrum is under examination, the limited resolution of the intensity contour plot, as well as the almost complete removal of overlap, makes the precise size and position of individual peaks less critical, so that a larger error in the intensity and frequency of the simulated spectrum is tolerable. Since a higher precision requirement would easily increase the computing load dramatically, it is necessary to analyze quantitatively the error introduced by ignoring the off-diagonal elements left in the H matrix (this will be discussed in § 4.2.1).

Therefore, there are many situations where coupling terms are too strong to be ignored at the beginning, but the diagonalization process can be truncated at certain points and may still give excellent results for comparison with experimental data.

Section 3 Direct Product Method

The density operator expressions of an nmr experiment shown in the previous section usually need to be represented in matrix form to calculate explicitly numerical values for spectral lines. Theoretically, any complete set of orthogonal base operators can be used to expand the density operator, and any complete set of orthogonal base functions can be used to expand these operators in matrix form[2]. The particular selection depends on the particular problem under discussion. The spin product operators { Bs }[8], generated from the spin angular momentum operators I_{kx}, I_{ky}, and I_{kz} of the individual spins, lead to elegant expressions in many cases. Other operator sets, such as spin polarization operators, single transition operators, single transition shift operators, etc., work well in many other cases. But all these operator sets are designed to simplify the quantum mechanical expressions of various nmr experiments. To obtain the matrix representation of these operators one usually needs extra calculations which often are not straightforward. The direct product method discussed in this section is a scheme particularly designed to simplify this job.

It is not a new idea to use the direct product method in the calculation of the matrix representation of these operators, and the value of this method for simplifying matrix calculations was recognized a long time ago[13,17]. But it is interesting that, to the knowledge of the author, it has only been used in the simple example-calculations of operator expressions, such as the Hamiltonian matrix of systems with up to three or four spins, the pulse rotation matrix, or the precession rotation matrix. In the numerical calculations of larger systems, instead of the direct product method, other general formulae[18,19] were used in practice. One reason for this phenomena is perhaps that, the matrices created by those general formula often have good properties. For example, the Hamiltonian matrix calculated by the methods in ref.[18] is block diagonal. This block diagonal form is a consequence of the fact that the sequence of the base spin product functions are listed according to their F_z numbers. The definition of the Hamiltonian operator guarantees that all its elements relating two states with different F_z numbers are zero. Therefore the size of the matrix which needs to be diagonalized becomes much reduced. This of course is highly desirable. But since the number of the states increases exponentially with the number of spins in the system, even if the matrix is block diagonal, the size of the largest block is

still increasing exponentially with the number of spins. That is why the calculation of these matrices needs to be further simplified.

When the matrix of these operators is calculated by the direct product method, they lose the block diagonal appearance. However, due to the intrinsic symmetry of direct multiplication, a matrix obtained this way has new properties which leads to simpler results, making it possible to calculate matrix elements by a group of recursive formulae.

§ 3.1.1 Direct Product Notation

A matrix **C**, of the size of (I·K × J·L), is defined as the direct product of two matrices **A** (size of I×J) and **B** (size of K×L), if its elements are created by the formula

$$c_{(i-1)K+k,\ (j-1)L+l} \equiv a_{i,j} \cdot b_{k,l} \qquad [3.1]$$

and is written as

$$\mathbf{C} \equiv \mathbf{A} \otimes \mathbf{B} \qquad [3.2]$$

To simplify the notation, bold exponents are used to represent the multiple direct product of k identical matrices:

$$\mathbf{C}^{\mathbf{k}} \equiv \mathbf{C} \otimes \mathbf{C} \otimes \ldots \otimes \mathbf{C} \qquad [3.3]$$

It should be noted that the above product is completely different than that of ordinary multiplication of k matrices:

$$\mathbf{C}^{k} \equiv \mathbf{C} \cdot \mathbf{C} \cdot \ldots \cdot \mathbf{C} \qquad [3.4]$$

The direct multiplication is order dependent. For example, all the following expressions represent the direct product of three matrices **A** and one matrix **E**, but in different multiplication sequence, hence giving different results:

$$\mathbf{A}^{\mathbf{3}}\ \mathbf{E}^{\mathbf{1}} = \mathbf{A} \otimes \mathbf{A} \otimes \mathbf{A} \otimes \mathbf{E}$$

$$\mathbf{A}^{\mathbf{2}}\,\mathbf{E}^{\mathbf{1}}\,\mathbf{A}^{\mathbf{1}} = \mathbf{A} \otimes \mathbf{A} \otimes \mathbf{E} \otimes \mathbf{A}$$

$$\mathbf{A}^{\mathbf{1}}\,\mathbf{E}^{\mathbf{1}}\,\mathbf{A}^{\mathbf{2}} = \mathbf{A} \otimes \mathbf{E} \otimes \mathbf{A} \otimes \mathbf{A}$$

$$\mathbf{E}^{\mathbf{1}}\,\mathbf{A}^{\mathbf{3}} = \mathbf{E} \otimes \mathbf{A} \otimes \mathbf{A} \otimes \mathbf{A} \qquad [3.5]$$

The four direct products in Eq. [3.5] can be further abbreviated as $\mathbf{A}^{(3)}\,\mathbf{E}^{(1)}$. That is, an exponent enclosed in parentheses represents all the possible permutations of directly multiplied matrix

sequences. Obviously, the total number of the possibilities of different multiplication sequences can be calculated by combination theory. For example, the number of the different direct products resulting from m matrices **A** and n matrices **B** is

$$N(\mathbf{A}^{(m)}\mathbf{B}^{(n)}) = C^{m}_{m+n} = (m+n)!/(m!n!) \qquad [3.7]$$

When the exponent equals 1, it will be omitted in obvious cases.

§ 3.1.2 Matrices For Spin Angular Momentum

As most of the following discussion involves I=1/2 spin systems, we will introduce four letters for the four Pauli matrices of a single spin:

$$\mathbf{E} = \begin{bmatrix} 1 & 0 \\ 0 & 1 \end{bmatrix} \qquad \mathbf{X} = \begin{bmatrix} 0 & 1 \\ 1 & 0 \end{bmatrix}$$

$$\mathbf{Y} = \begin{bmatrix} 0 & -i \\ i & 0 \end{bmatrix} \qquad \mathbf{Z} = \begin{bmatrix} 1 & 0 \\ 0 & -1 \end{bmatrix} \qquad [3.8]$$

Please note that these matrices differ from the Pauli matrices by a factor of 1/2. This is to avoid having this factor multiplied to its power in the direct product expressions, hence the values of non-zero elements of Pauli matrices are changed to one, and the factor 1/2 is multiplied at the beginning of each expression, as shown in the following examples:

$$\mathbf{E}^2 = \mathbf{E} \otimes \mathbf{E} = \begin{bmatrix} 1 & 0 & 0 & 0 \\ 0 & 1 & 0 & 0 \\ 0 & 0 & 1 & 0 \\ 0 & 0 & 0 & 1 \end{bmatrix} \qquad [3.9]$$

$$\mathbf{X}^2 = \mathbf{X} \otimes \mathbf{X} = \begin{bmatrix} 0 & 0 & 0 & 1 \\ 0 & 0 & 1 & 0 \\ 0 & 1 & 0 & 0 \\ 1 & 0 & 0 & 0 \end{bmatrix} \qquad [3.10]$$

$$\mathbf{X}^{1}\mathbf{E}^{1}=\mathbf{X}\otimes\mathbf{E}=\begin{bmatrix}0&0&1&0\\0&0&0&1\\1&0&0&0\\0&1&0&0\end{bmatrix} \qquad [3.11]$$

$$\mathbf{X}\otimes\mathbf{Y}+\mathbf{Y}\otimes\mathbf{X}=\begin{bmatrix}0&0&0&-i\\0&0&i&0\\0&-i&0&0\\i&0&0&0\end{bmatrix}+\begin{bmatrix}0&0&1&-i\\0&0&-i&1\\0&i&0&0\\i&0&0&0\end{bmatrix}$$

$$=2\begin{bmatrix}0&0&0&-i\\0&0&0&0\\0&0&0&0\\i&0&0&0\end{bmatrix} \qquad [3.12]$$

$$\mathbf{X}\otimes\mathbf{X}+\mathbf{Y}\otimes\mathbf{Y} = \begin{bmatrix} 0 & 0 & 0 & 1 \\ 0 & 0 & 1 & 0 \\ 0 & 1 & 0 & 0 \\ 1 & 0 & 0 & 0 \end{bmatrix} + \begin{bmatrix} 0 & 0 & 0 & -1 \\ 0 & 0 & 1 & 0 \\ 0 & 1 & 0 & 0 \\ -1 & 0 & 0 & 0 \end{bmatrix}$$

$$= 2 \begin{bmatrix} 0 & 0 & 0 & 0 \\ 0 & 0 & 1 & 0 \\ 0 & 1 & 0 & 0 \\ 0 & 0 & 0 & 0 \end{bmatrix} \qquad [3.13]$$

$$\mathbf{E}\otimes\mathbf{Z}+\mathbf{Z}\otimes\mathbf{E} = \begin{bmatrix} 1 & 0 & 0 & 0 \\ 0 & -1 & 0 & 0 \\ 0 & 0 & 1 & 0 \\ 0 & 0 & 0 & -1 \end{bmatrix} + \begin{bmatrix} 1 & 0 & 0 & 0 \\ 0 & 1 & 0 & 0 \\ 0 & 0 & -1 & 0 \\ 0 & 0 & 0 & -1 \end{bmatrix}$$

$$= 2 \begin{bmatrix} 1 & 0 & 0 & 0 \\ 0 & 0 & 0 & 0 \\ 0 & 0 & 0 & 0 \\ 0 & 0 & 0 & -1 \end{bmatrix} \qquad [3.14]$$

$$\mathbf{Z} \otimes \mathbf{Z} + \mathbf{X} \otimes \mathbf{X} = \begin{bmatrix} 1 & 0 & 0 & 0 \\ 0 & -1 & 0 & 0 \\ 0 & 0 & -1 & 0 \\ 0 & 0 & 0 & 1 \end{bmatrix} + \begin{bmatrix} 0 & 0 & 0 & 1 \\ 0 & 0 & 1 & 0 \\ 0 & 1 & 0 & 0 \\ 1 & 0 & 0 & 0 \end{bmatrix}$$

$$= \begin{bmatrix} 1 & 0 & 0 & 1 \\ 0 & -1 & 1 & 0 \\ 0 & 1 & -1 & 0 \\ 1 & 0 & 0 & 1 \end{bmatrix} \qquad [3.15]$$

At this point we can define

$$\mathbf{V}_k = \mathbf{E}^{n-k+1}\,\mathbf{V}^1\,\mathbf{E}^{k-1} \qquad [3.16]$$

where $\mathbf{V} = \mathbf{X}$, $\mathbf{Y}$, or $\mathbf{Z}$, and n is the number of spins in the system. Similarly,

$$\mathbf{V}_k\,\mathbf{W}_j = \mathbf{E}^{n-k+1}\,\mathbf{V}^1\,\mathbf{E}^{k-j}\,\mathbf{W}^1\,\mathbf{E}^{j-1} \qquad [3.17]$$

where both $\mathbf{V}$ and $\mathbf{W} = \mathbf{X}$, $\mathbf{Y}$, or $\mathbf{Z}$.

These new definitions represent more than a compressed notation, and have several characteristics. First, compared with Cartesian spin angular momentum operators for a spin system, a numerical factor with different values is necessary for the latter, such as I_x, $2I_{x1}I_{x2}$, $4I_{z1}I_{z2}I_{z3}$, $8I_{z1}I_{z2}I_{x3}I_{y4}$, etc. While in the direct product notation, all these factors are replaced by 1/2: $1/2\mathbf{X}$, $1/2\mathbf{X}^1$, $1/2\mathbf{Z}^3$, $1/2\mathbf{Y}^1\,\mathbf{X}^1\,\mathbf{Z}^2$, etc. Second, the Cartesian spin angular momentum operators do not provide the information of the number of spins in the system. $2I_{x1}I_{x2}$ can be the product of the x component of spin 1 and spin 2 in a system containing any number of spins. Therefore, with an expression written in these operators, such as a Hamiltonian expression, without specifying how many spins are in this system, no matrix representation can be created. But in the direct product notation, the number of spins equal the

number of single spin symbols. So $2I_{x1}I_{x2}$ will be symbolized as $1/2\mathbf{X}^1\,\mathbf{X}^1 = 1/2\mathbf{XX}$ (here the exponent 1 is omitted, the same omission will be applied hereafter) for a two-spin system; **1/2EXX** for a three-spin system, **1/2EEEEXX** for a six-spin system, etc. Using these expressions, the matrix representation can be written down immediately without any calculation, e.g.:

1/2EXX = 1/2

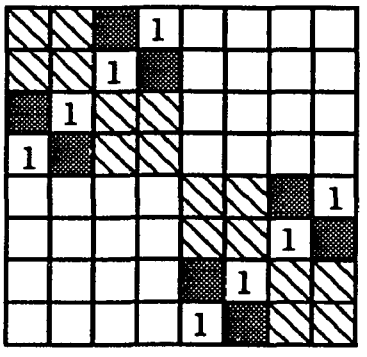

[3.18a]

1/2 XXE = 1/2

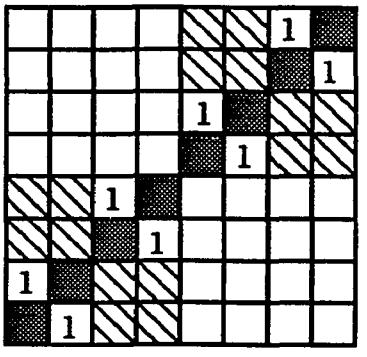

[3.18b]

$1/2\,\mathbf{EEXX} = 1/2$ 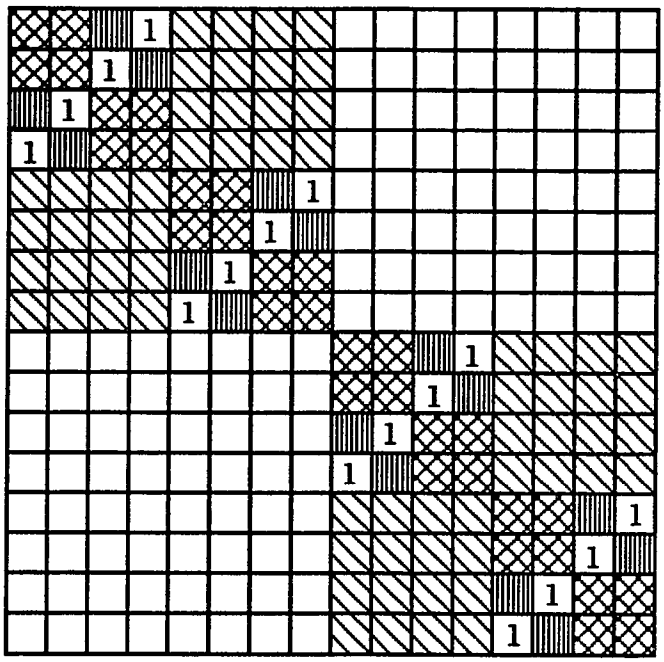 [3.19]

In the above matrices, the nonzero elements of each single spin matrix were shaded, to show that calculation is not necessary.

§ 3.2 Various Matrices Calculated by the Direct Product Method

§ 3.2.1 Receiver matrix F^+

By definition, $F^+ = \Sigma\, I_{kx} + iI_{ky}$. Translating this expression into direct product notation,

$$F^+ = F_x + iF_y = 1/2\, \Sigma_k\, (\mathbf{X}_k + i\mathbf{Y}_k)$$

$$= 1/2\, (\mathbf{EEEX} + \mathbf{EEXE} + \mathbf{EXEE} + \mathbf{XEEE} +$$

$$= \quad i\, (\mathbf{EEEY} + \mathbf{EEYE} + \mathbf{EYEE} + \mathbf{YEEE})) \qquad [3.20]$$

Using Eqs. [3.16, 3.17, 3.20], the matrix representation can be obtained and has the form shown in Fig 3.1:

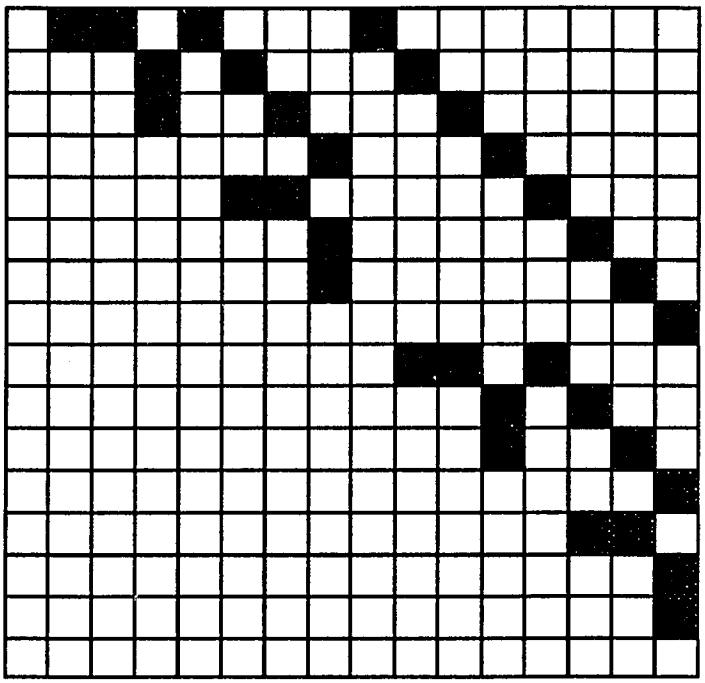

Fig 3.1 F^+ matrix of a four-spin system.

Shaded elements = 1, all other elements = 0

§ 3.2.2 Hamiltonian Matrix H

Again, the operator's definition is first written down, then translated into the direct product notation:

$$H = \Sigma_k \omega_k I_{zk} + \Sigma_{k>l} J_{kl} I_k I_l$$

$$= 1/2 \Sigma_k \omega_k \mathbf{Z}_k + 1/2^2 \Sigma_{k>l} J_{kl}(\mathbf{X}_k\mathbf{X}_l + \mathbf{Y}_k\mathbf{Y}_l + \mathbf{Z}_k\mathbf{Z}_l) \qquad [3.21]$$

for a four-spin system the matrix can be obtained as indicated in Fig 3.2:

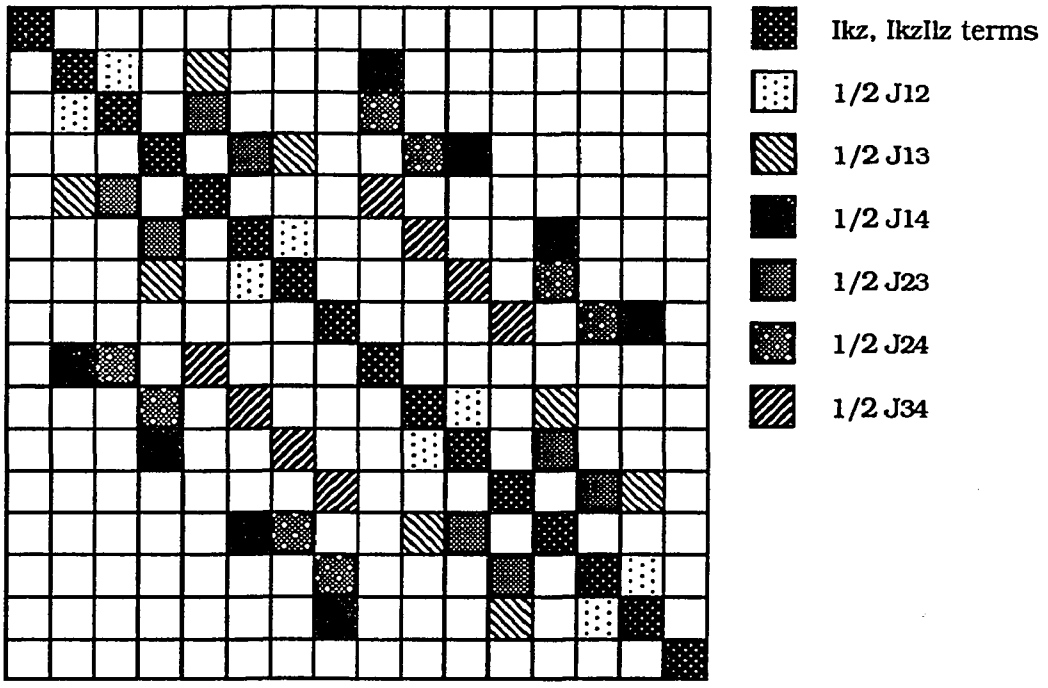

Fig 3.2 H matrix of a four-spin system.

Note that the H matrix is not in a block-diagonal form. That is

because the sequence of the state functions is not listed according to Fz number. Instead, they are listed according to the binary number code of the spin state functions, where for a spin up (α) means '0' and a spin down (β) means '1'. That is, '0010' represents the state $|\alpha\alpha\beta\alpha>$, and the sequence number of this state is '0010', or 2; and the sequence number of state $|\alpha\beta\beta\beta>$ will be '0111', or 7. From Fig 3.2 it can be seen that the positions of off-diagonal elements reflect clearly the fact that they come from the cross coupling terms in the definition of the Hamiltonian.

As mentioned before, the block-diagonal appearance of the Hamiltonian matrix created according to F_z sequence of the function states matches the desire of compressing the matrix size as much as possible. However, once the matrix is created by the direct product method, its highly symmetrical appearance makes the requirement of storing the whole matrix as a two dimensional array disappear, as will be explained in section 4.

§ 3.2.3 Eigenvector Matrix T

The most important advantage of the direct product notation is its convenience in describing the Jacobi transformation process. The total process is a successive series of orthogonal rotations, in which each step eliminates one group of off-diagonal elements, as well as modifies the values of all the elements sharing either their row or column numbers with the elements being eliminated. It can be shown that the sum of the squares of the off-diagonal elements decreases monotonically with each step of the transformation[15], but is bounded below by zero, so the convergence is guaranteed. The process can be terminated when the largest off-diagonal elements are less than a pre-specified threshold.

When the Hamiltonian matrix is expanded in the spin-product function space, the sequence of these state functions determines the appearance of the matrix. In the total-quantum-number-sequence, the matrix is block-diagonal, and a natural way to diagonalize it is to transform each block separately, as the program LAOCN does[16]. If the binary-code-sequence is chosen, as in the matrix created by direct product method, the fact that all the off-

diagonal elements belonging to the same coupling term can be eliminated simultaneously is more obvious and hence is more easily realized. Therefore it leads the way to a new algorithm.

The off-diagonal elements in a Hamiltonian matrix (Eqs.3.21) are $1/2^2 \sum_{k>l} J_{kl}(\mathbf{X}_k\mathbf{X}_l + \mathbf{Y}_k\mathbf{Y}_l)$. For an N-spin system, these elements are divided into N(N-1)/2 groups, each group contains 2^{N-2} pairs of elements of value $J_{kl}/2$ before the Jacobi transformation begins. The rotation matrix to eliminate all these elements can be specified as

$$T_{kl} = 1/2[\mathbf{E}_k\mathbf{E}_l\,(1 + \cos\phi_{kl}) + \mathbf{Z}_k\mathbf{Z}_l\,(1 - \cos\phi_{kl}) + (\mathbf{X}_k\mathbf{X}_l + \mathbf{Y}_k\mathbf{Y}_l)\sin\phi_{kl}] \qquad [3.22]$$

where ϕ_{kl} is a vector with 2^{N-2} components, and each is determined by

$$(\phi_{kl})_m = 1/2\,\tan^{-1}(J_{kl}/\Delta D_{kl})_m,\ m=1, 2, \ldots, 2^{N-2} \qquad [3.23]$$

where ΔD_{kl} is the difference of diagonal elements, and all these 2^{N-2} J_{kl} values are the same at the beginning. As the transformation goes on step by step, some off-diagonal elements belonging to the same coupling term no longer share the same value, and then the $(\phi_{kl})_m$ rotation angles also deviate from each other, as illustrated in Fig 3.3, 3.4, and 3.5.

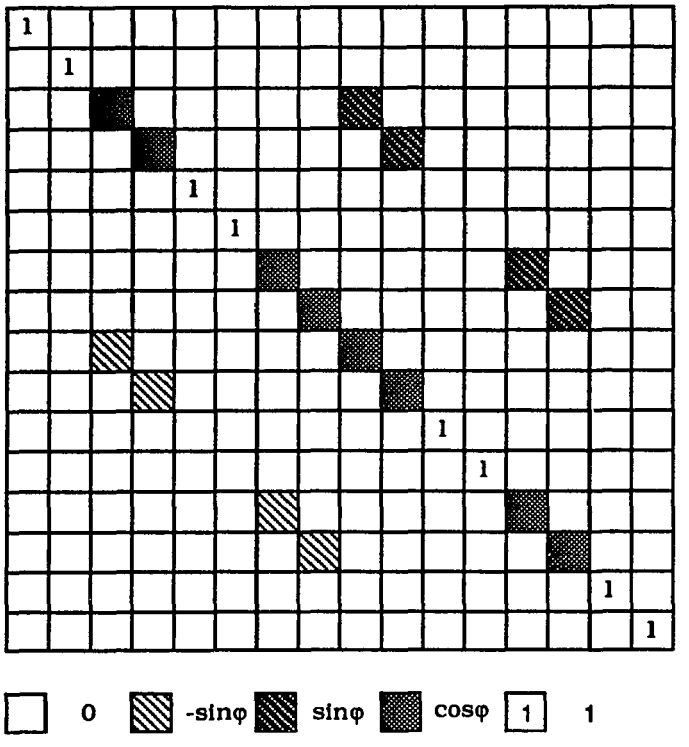

Fig 3.3 T_{24} matrix of a four-spin system

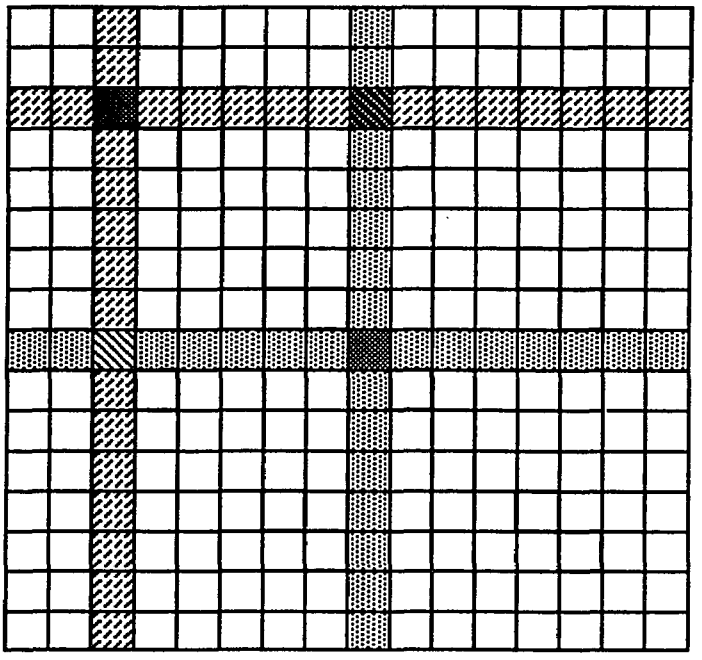

Fig 3.4 All the elements sharing row or colume number with the first pair off-diagonal elements of J24 will change values during the first rotation of T24.

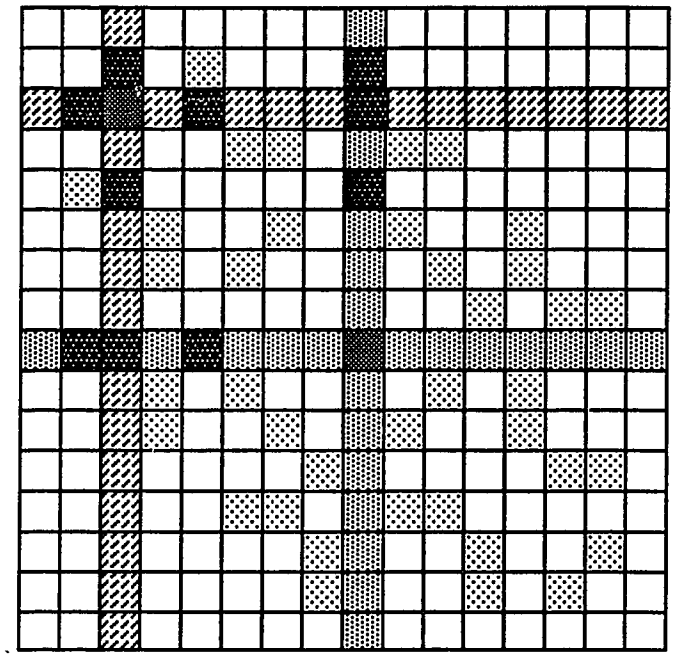

non-zero elements of H matrix.

off-diagonal elements whose value changed.

Fig 3.5 All the off-diagonal elements of H matrix sharing row or column number with the first pair off-diagonal elements of J24 will change values during the first rotation of T24. These elements are shaded with darkest color.

As mentioned before, such a rotation will not only eliminate the J_{kl} elements, it will also change the values of all the elements sharing row or column numbers with J_{kl} elements. All these elements belong to J_{km} and J_{lm} coupling pairs, with m = 1, 2, ..., N but m ≠ k or l. Their values are to be updated by the following formula:

$$[(J_{km})_{i+1}]_j = [(J_{km})_i \cos\phi_{kl} \pm (J_{lm})_i \sin\phi_{kl}]_j \qquad [3.24]$$

where m = 1, 2, ..., N but m ≠ k or l; j = 1, 2, ..., 2^{N-2} is the index of the off-diagonal elements belonging to one coupling pair; i and i+1 mean the values after the i-th and (i+1)-th Jacobi transformations, respectively.

The total eigenvector matrix is the product of all these T_i, until the largest absolute off-diagonal value, after i_m-th rotation, is less than the threshold:

$$T = \prod_i T_i. \qquad [3.25]$$

§ 3.3 Notation for the Density Matrix

Encouraged by the simplicity in the Hamiltonian expression, a similar notation for the density matrix σ is designed as follows.

First, in order to locate every single element in σ, four basic matrices, each having only one non-zero element, are defined for the I=1/2 spins,

$$\mathbf{u} = \begin{bmatrix} 1 & 0 \\ 0 & 0 \end{bmatrix} \qquad \mathbf{d} = \begin{bmatrix} 0 & 0 \\ 0 & 1 \end{bmatrix}$$

$$\mathbf{p} = \begin{bmatrix} 0 & 1 \\ 0 & 0 \end{bmatrix} \qquad \mathbf{m} = \begin{bmatrix} 0 & 0 \\ 1 & 0 \end{bmatrix} \qquad [3.26]$$

which when combined with the identity matrix **E**, make it very convenient to express the elements of σ of any N-spin system, as for example,

$\mathbf{E^2 p^1}$ =

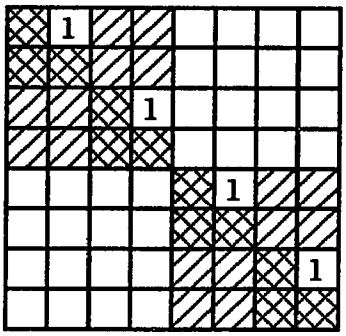

[3.27]

$\mathbf{E^1 p^2}$ =

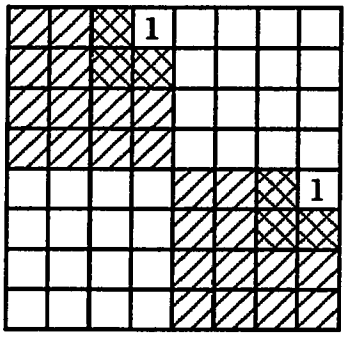

[3.28]

$\mathbf{p}^3 =$ 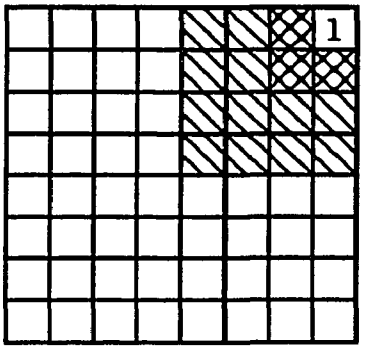 [3.29]

$\mathbf{p}^{(2)}\mathbf{m}^{(1)} = \begin{pmatrix} \mathbf{p}^2\mathbf{m}^1 \\ \mathbf{p}^1\mathbf{m}^1\mathbf{p}^1 \\ \mathbf{m}^2\mathbf{p}^1 \end{pmatrix} =$ 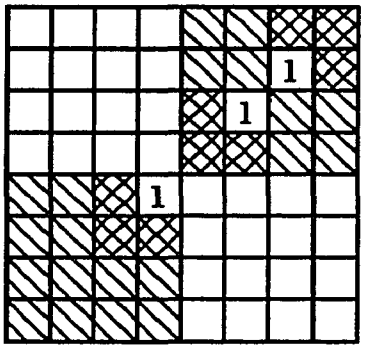 [3.30]

The non-zero elements in each matrix within these direct product expressions are shaded, so it can be seen that the final results were obtained with no calculation.

Eqs. [3.27-29] represent respectively the coherences of single, double, and triple quantum transitions with order +1. Eq.[3.27] and Eq.[3.30] both refer to single quantum transitions (SQT), but with the difference that $\mathbf{E}^2\mathbf{p}^1$ refers to the transitions of spin 1 only, and $\mathbf{p}^{(2)}\mathbf{m}^{(1)}$ refers to the combined transition of all three spins

simultaneously, with two spins flipped up and one spin flipped down, and hence the quantum number F_z is still changed by one. For a three-spin system, $\mathbf{E}^{(2)}\mathbf{p}^{(1)}$ and $\mathbf{E}^{(2)}\mathbf{m}^{(1)}$ represent all the single spin single quantum transitions of order +1 and -1 respectively:

$$\mathbf{E}^{(2)}\,\mathbf{P}^{(1)} = \begin{pmatrix} \mathbf{E}^2\mathbf{P}^1 \\ \mathbf{E}^1\mathbf{P}^1\mathbf{E}^1 \\ \mathbf{P}^1\mathbf{E}^2 \end{pmatrix} =$$

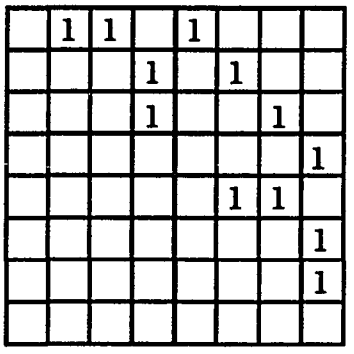

[3.31]

$$\mathbf{E}^{(2)}\,\mathbf{M}^{(1)} = \begin{pmatrix} \mathbf{E}^2\mathbf{M}^1 \\ \mathbf{E}^1\mathbf{M}^1\mathbf{E}^1 \\ \mathbf{M}^2\mathbf{E}^1 \end{pmatrix} =$$

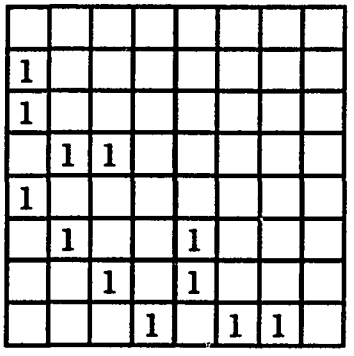

[3.32]

The total observable coherences with order +1 are those direct products with one more **p** than **m**, and the rest all **E**'s:

$$\mathbf{E}^{(2)}\,\mathbf{P}^{(1)} \quad + \quad \mathbf{P}^{(2)}\,\mathbf{M}^{(1)} \quad =$$

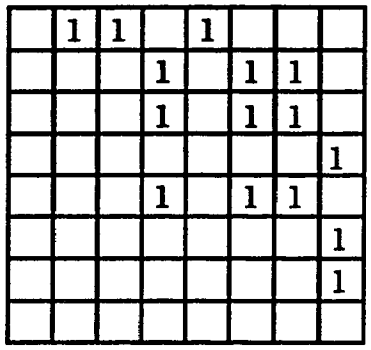

[3.33]

Eq.[3.33] shows that there are 15 observable coherences with order +1 for a three-spin system. That is also the largest number of spectral lines of its 1D spectrum. Expressions like Eq.[3.33] can generally be used to count the largest number of spectral lines to be expected. For example, for the SQT of a ten-spin system we have

$$[\mathrm{SQT}]^{+1} = \mathbf{E}^{(9)}\mathbf{p}^{(1)} + \mathbf{E}^{(7)}\mathbf{p}^{(2)}\mathbf{m}^{(1)} + \mathbf{E}^{(5)}\mathbf{p}^{(3)}\mathbf{m}^{(2)} +$$

$$+ \mathbf{E}^{(3)}\mathbf{p}^{(4)}\mathbf{m}^{(3)} + \mathbf{E}^{(1)}\mathbf{p}^{(5)}\mathbf{m}^{(4)} \qquad [3.34]$$

Therefore the 1D spectrum of a ten-spin system at most can have

$$N[\mathrm{SQT}]^{+1} = C_{10}^{1}2^{9} + C_{10}^{1}C_{9}^{2}2^{7} + C_{10}^{2}C_{8}^{3}2^{5} +$$

$$+ C_{10}^{3}C_{7}^{4}2^{3} + C_{10}^{4}C_{6}^{5}2^{1} = 167{,}960 \qquad [3.35]$$

lines. Similarly, the number of DQT (double quantum transitions), TQT (triple quantum transitions), etc. can also be calculated by the same method.

Finally, for an N=1 spin system, there is a one to one correspondence between our symbols and the polarization operators:

$$I^{\alpha} = \mathbf{u}, \qquad I^{\beta} = \mathbf{d}, \qquad I^{+} = \mathbf{p}, \qquad I^{-} = \mathbf{m} \qquad [3.36]$$

When $N \neq 1$, a subscript can be used in the polarization operators to label the different elements in the σ matrix, but with the direct product notation, the position of individual element can be explicitly spelled out (again, the shaded area represents a non-zero element of each single-spin matrix symbol):

mdddpp = 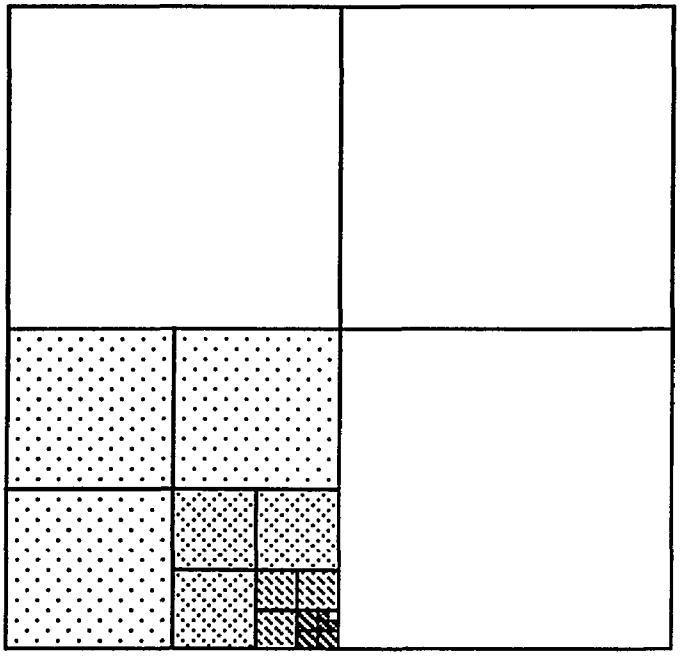 = $\sigma_{61,32}$

upd = 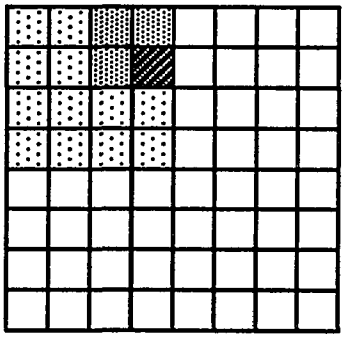 = $\sigma_{2,4}$ [3-37]

From the examples shown above, it should be clear that the direct product notation relates various operators and their matrix representations. Therefore, any expression written using these operators, when translated into the direct product notation, gives the matrix representation immediately. Since all nmr experiments can be described by such operator expressions, their matrix form can be obtained by just replacing the operators with the corresponding direct product symbols.

Section 4 SSSQT - Single Spin Single Quantum Transitions

§ 4.1 SSSQT and Their Corresponding Spectral Lines

In the last section we introduced the direct product notation $\mathbf{E}^{(N-1)}\mathbf{p}^{(1)}$ and $\mathbf{E}^{(N-1)}\mathbf{m}^{(1)}$, for SSSQT of order +1 and -1 respectively. They can also be written as $\{\mathbf{p}_k\}$ and $\{\mathbf{m}_k\}$, k=1, 2, ..., N. Since $\mathbf{p}_k$ represents the transition of spin k from $|\beta\rangle$ to $|\alpha\rangle$ while all other (N-1) spins keep their states unchanged; and $\mathbf{m}_k$ represents a transition from $|\alpha\rangle$ to $|\beta\rangle$.

In a 1D spectrum, if the weak coupling condition holds for all the coupling pairs, these SSSQT, or $\{\mathbf{p}_k\}$, correspond to the spectral lines located at $\omega_k \pm 1/2J_{km}$, m=1, 2, ..., N but $m \neq k$; and k=1, 2, ..., N. There are the same number of lines corresponding to $\{\mathbf{m}_k\}$, located at the other side of the ω=0 axis. Whether it is valid to say that the coupling is weak depends on the ratio $\mu = |J_{kl}/(\omega_k-\omega_l)|$ and the precision required. When it is valid to do so, the SSSQT are taken as the whole spectrum, and all combined lines are omitted, as their intensities are below the noise threshold used to judge the

weakness of the couplings. Fig 4.1 shows the 12 SSSQT lines of a three-spin system, with their corresponding density matrix elements expressed as the direct product of single spin matrices.

From Fig 4.1, it is clear that SSSQT carries the information necessary to complete the assignment. In a 2D spectrum, the COSY cross peaks between two SSSQT lines of two different dimensions tell us the topology of the coupling network, and from the splitting of the peaks the coupling constant can be measured. Therefore, most, if not all, of the structural information obtainable from an nmr spectrum, can be obtained through SSSQT peaks. Even in an experiment where multiple quantum filters are used to edit the spectrum, in most situations, the final plot is still made of SSSQT peaks.

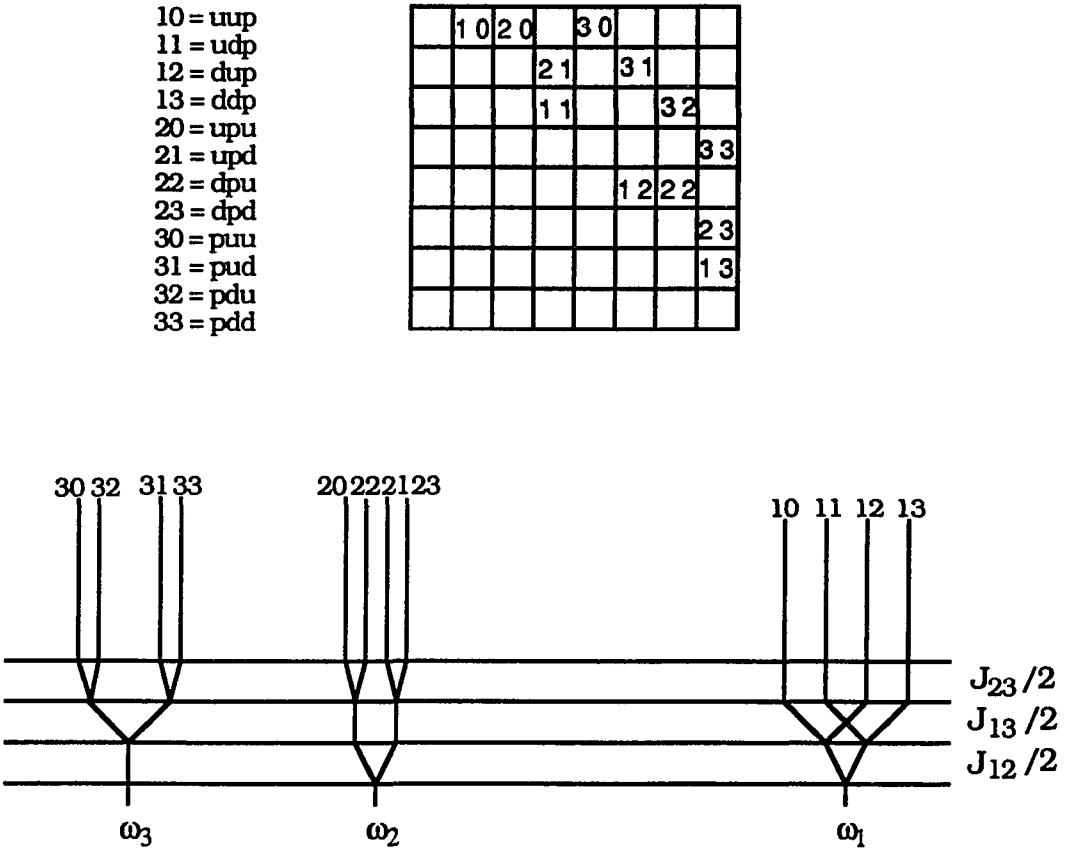

Fig 4.1 SSSQT of a three-spin (I = 1/2) system. When the density matrix is created by the direct product method, every SSSQT spectral line can be labeled uniquely by **m**, **p**, **d**, **u** symbols.

§ 4.2.1 A Quantitative analysis of a two-spin system

Under the weak coupling assumption, SSSQT represents the entire spectrum. For an N-spin system, there could be as many as $N2^{N-1}$ SSSQT lines, however, the real spectrum has fewer peaks due to spectral overlap.

When strong coupling exists, the H matrix must be diagonalized to such a point that any further off-diagonal elements left are small enough to be ignored. The effect of the Jacobi transformation is that it will change the frequencies as well as intensities of the simulated spectral lines. Qualitatively, these effects can be demonstrated through a two-spin example, as shown in Fig 4.2.

In Fig 4.2, when the coupling J_{12} is weak, the H matrix elements have the following values:

$$D_1 = H_{11} = 1/2[+ \omega_1 + \omega_2 + J/2]$$

$$D_2 = H_{22} = 1/2[- \omega_1 + \omega_2 - J/2]$$

$$D_3 = H_{33} = 1/2[+ \omega_1 - \omega_2 - J/2]$$

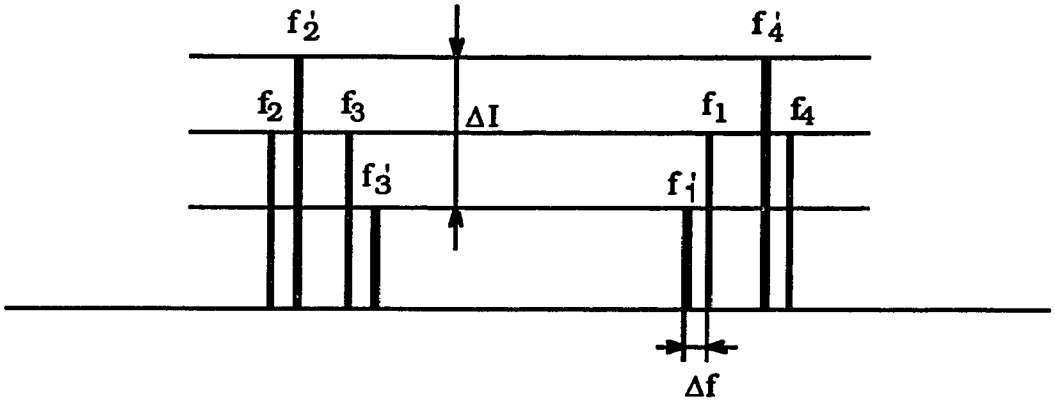

D_1			
	D_2	J/2	
	J/2	D_3	
			D_4

	f_1	f_2	
			f_3
			f_4

Fig 4.2 The H and σ matrices of a two-spin system. D's are diagonal elements of the H matrix. If J is much less than Δw, the intensities of the four lines f1~f4 are almost equal; if J is too large to be neglected, the H matrix must be diagonalized, and the spectral lines would look like f '1~f '4 as shown in the picture.

$$D_4 = H_{44} = 1/2[- \omega_1 - \omega_2 + J/2] \qquad [4.1]$$

Off-diagonal elements are omitted. The positions of the spectral lines $f_1 \sim f_4$ are:

$$f_1 = D_1 - D_2 = \omega_1 + J/2$$

$$f_2 = D_1 - D_3 = \omega_2 + J/2$$

$$f_3 = D_2 - D_4 = \omega 2 - J/2$$

$$f_4 = D_3 - D_4 = \omega_1 - J/2 \qquad [4.2]$$

When coupling is strong, $H_{23} = H_{32} = J/2$ is not negligible, and the H matrix needs to be diagonalized. The effect of the diagonalization is calculated as follows:

$$D'_1 = D_1$$

$$D'_2 = D_2 \cos^2\phi + D_3 \sin^2\phi - \sin 2\phi\, J/2$$

$$D'_3 = D_3 \cos^2\phi + D_2 \sin^2\phi + \sin 2\phi\, J/2$$

$$D'_4 = D_4 \qquad [4.3]$$

In the simulated spectrum, the effect is $f_1 \sim f_4$ are moved to $f'_1 \sim f'_4$ (see Fig 4.2). The shift of peak f_1, i.e., Δf, can be calculated as

$$\Delta f = f'_1 - f_1$$

$$= (D'_{1'} - D'_2) - (D_1 - D_2)$$

$$= D_2 - D_{2'}$$

$$= \sin 2\phi (D_2 - D_3) + \sin 2\phi \, J/2$$

$$= \Delta\omega/2 \, [2\sin^2\phi + \sin 2\phi \tan 2\phi]$$

$$= \Delta\omega/2[(1 + \mu^2)^{1/2} - 1] \qquad [4.4]$$

where $\phi = [\tan^{-1}(J/\Delta\omega)]/2$, is the Jacobi rotation angle, and $\mu = J/\Delta\omega = J/(\omega_2 - \omega_1)$ is the ratio of the coupling to the chemical shift difference between the two spins.

Not only the frequencies are changed, but the intensities change as well:

$$\Delta I = \Delta I_4 + \Delta I_1$$

$$= I(f'_4) - I(f_4) + I(f_1) - I(f'_1)$$

$$= I(f'_4) - I(f'_1)$$

$$= 2I_0 \sin\phi$$

$$= 2 \, I_0 \, [(1-(1 + \mu^2)^{-1/2}]^{1/2} \qquad [4.5]$$

Fig 4.3 summarizes the effect on both frequency and intensity. Generally, for a coupling of J~20 Hz, a negligible frequency shift (Δf < 1 Hz) requires $|\Delta\omega| > 4J \sim 80$ Hz; if J~5 Hz, this requirement is only $|\Delta\omega| > J \sim 5$ Hz. For an even smaller coupling, no requirement need be imposed on $|\Delta\omega|$. Since the intensity is more sensitive to the transformation, it is more important when a quantitative comparison is to be made between the simulated and experimental spectra[21,22]. Basically, it is not always safe to take a weak coupling assumption into the simulation without a careful analysis of the error that could be introduced.

The same reasoning implies that a 3D simulation, which emphasizes the frequency of the peaks, is more reliable when the weak coupling assumption may be assumed, because the intensity usually must be coded with lower resolution in a 3D plot. In the circumstances that the intensity must be quantitatively measured, weak coupling is only valid for those coupled pairs with μ smaller than 0.1, to avoid an error over ~10% in the intensity. For a modest coupling J~10 Hz, even for a 500 MHz machine, the required difference in chemical shifts of the coupled pair would be $\Delta\delta > 0.2$ ppm.

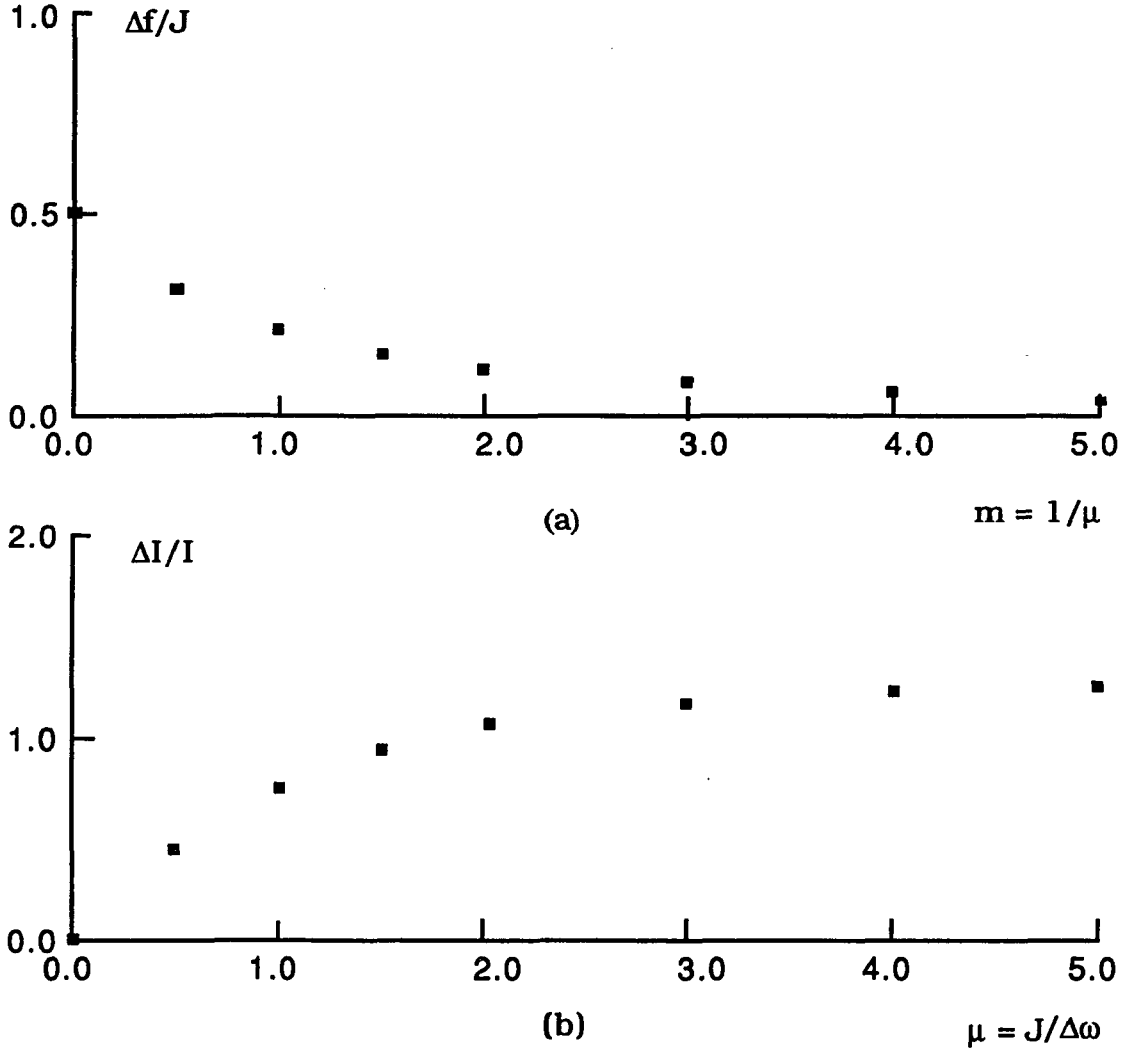

Fig 4.3 The effects on the frequency (a) and intensity (b) of the strong coupling. The definition of Δf and ΔI refers to Fig 4.2.

The above estimate was made analyzing a two-spin system. When more spins are included in the system, one spectral line could be coupled to many other lines, and the successive Jacobi rotations could possibly accumulate errors beyond a tolerable range.

In 2D simulation, the line shape problem would make the situation more complex, and a small error can change the appearance of the contour plot dramatically. Based on these considerations, the 2D simulation must take into account the whole numerical calculation of the density matrix, as the programs SPHINX and LINSHA do[20,21,22].

§ 4.2.2 Jacobi transformation for an n-spin system

Fig 4.4 shows the Jacobi transformation of a three-spin subsystem within an N-spin system. When spins i, j, and k are coupled together through J_{ij}, J_{ik}, and J_{jk}, and when off-diagonal elements of J_{ij} are being eliminated, the values of elements belonging to J_{ik} and J_{jk} will be modified according to

$$J'_{ik} = J_{ik}\cos\phi + J_{jk}\sin\phi$$

$$J'_{jk} = J_{jk}\cos\phi - J_{ik}\sin\phi \qquad [4.6]$$

$$J'_{ij} = 0$$

where J_{ij}, J_{ik}, and J_{jk} all have 2^{N-2} values (see Fig 4.4).

In Fig 4.4, we use arrows to describe the effect that after Jacobi rotation, half of the elements of J_{ik} were changed to ($J_{ik}\cos\phi + J_{jk}\sin\phi$), and the other half were changed to ($J_{ik}\cos\phi - J_{jk}\sin\phi$); the same is true for the elements of J_{jk}.

In Fig 4.5, the same effect was described for systems with 4, 5, and 6 spins. There each circle represents a spin, each line represents a coupling between two spins linked by that line. Similar

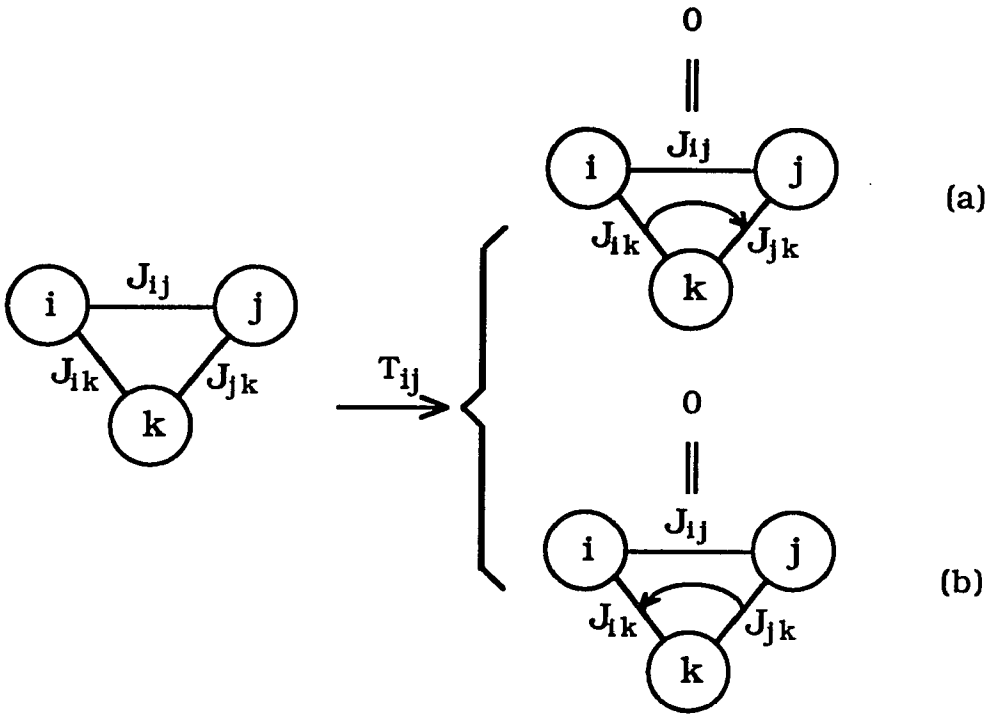

Fig 4.4 The effect of Jacobi rotation eliminating Jij on the values of Jik and Jjk. Curved arrows mean Eq. [4.6]. Circles mean spins, and each line between two circles means a coupled pair.

pictures can be designed for the σ and F^+ matrix. In order to relate these rules more tightly to the spectral lines, we draw all the $N2^{N-1}$ SSSQT lines for an N-spin system as the vertical lines in Fig 4.6, and label the shift in frequency made by the couplings as a solid(+) or empty(-) circles at the intersections of the vertical lines (Zeeman terms in the Hamiltonian operator) and horizontal lines (J coupling terms in the Hamiltonian operator). The arrows in Fig 4.6 have the same meaning as in Fig 4.5, i.e., the changes in intensities made by the Jacobi transformation. Fig 4.6 displayed the same thing as Fig 4.5, but with a different appearance. These pictures are equivalent to the recursive formula of the total Jacobi transformation process. All these relations are obvious only when the matrix is obtained by the direct product method.

In accord with Fig 4.5-4.6, the 1D spectrum of any N-spin system can be calculated efficiently.

A FORTRAN program, based on these recursive formulae, was developed and implemented on a microvax-II computer. It uses the rules of Fig 4.5 to eliminate the off-diagonal elements of the H matrix, stores the φ values for each Jacobi rotation, and uses them in the calculation of intensities by the rules explained in Fig 4.6.

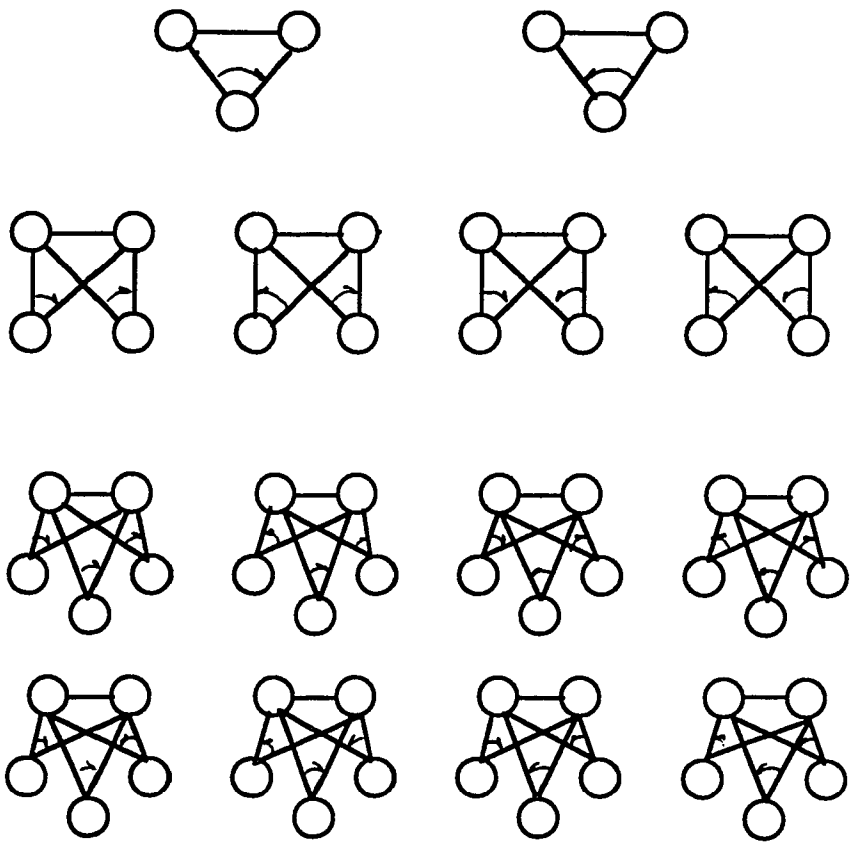

Fig 4.5a Coupling network of N = 3, 4, and 5 spin systems.

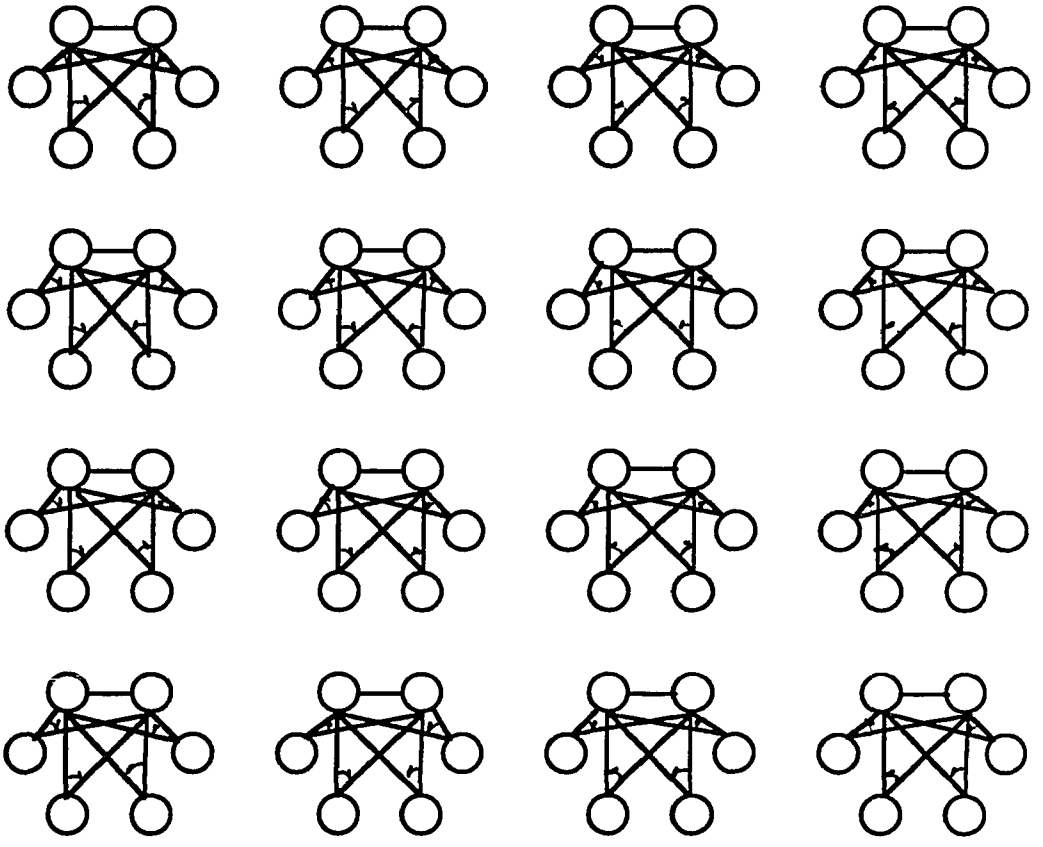

Fig 4.5b Coupling network of N = 6 spin systems.

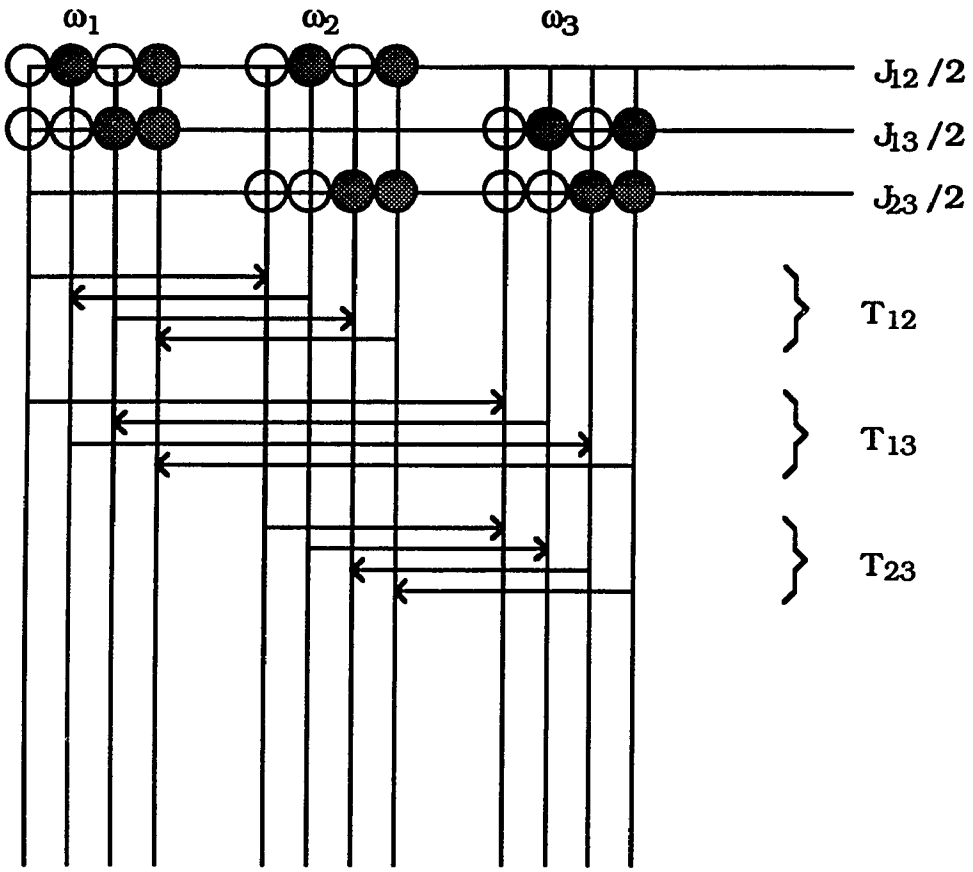

Fig 4.6a The effect of Jacobi rotation Tij on the SSSQT elements in the σ matrix for an N = 3 spin system. The arrows have a similar meaning to those in Fig 4.4, but here are applied to the intensity of the spectral lines shown.The white and gray circles on the intersections specify the frequency shift by an amount of + Jij/2 and -Jij/2, respectively.

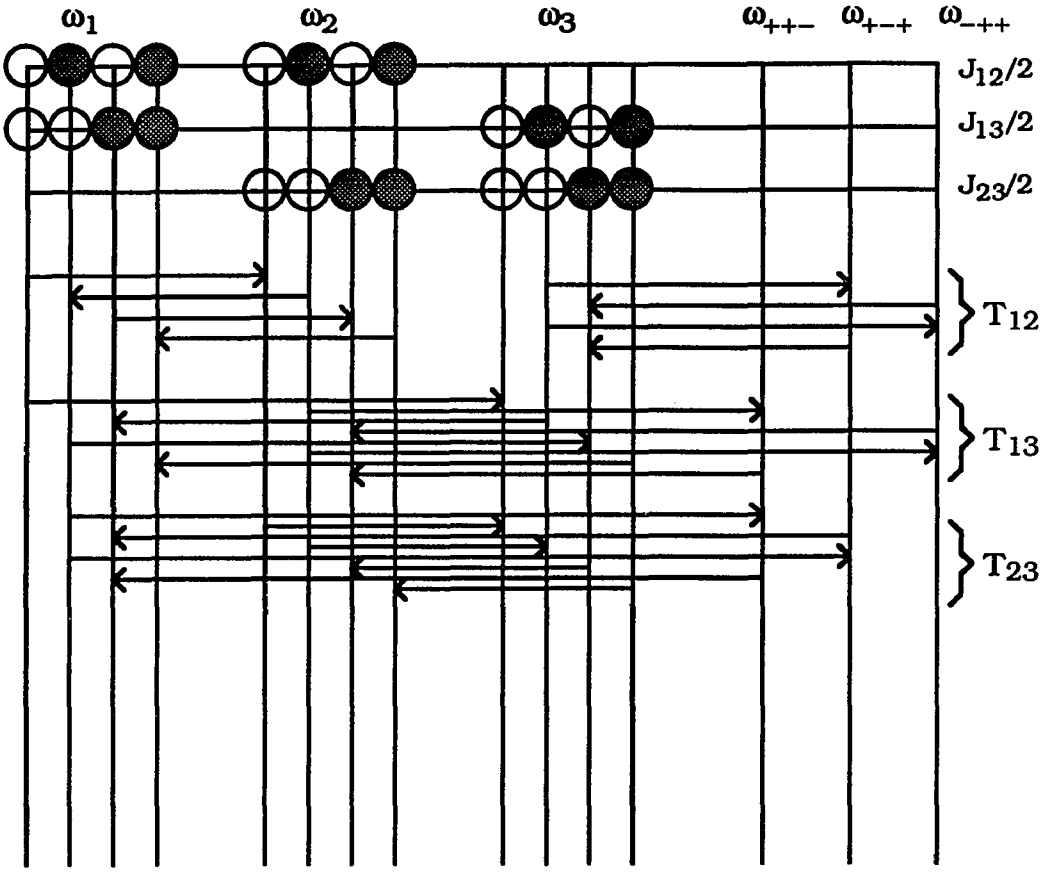

Fig 4.6 b The effect of Jacobi rotation Tij on the SQT elements in σ matrix for N=3 spin system.The arrows and the circles have a similar meaning as in Fig 4.6 a, ω-++, ω+-+, ω++- means -ω1+ω2+ω3, ω1-ω2+ω3, ω1+ω2-ω3, respectively.

In Fig 4.6 only the SSSQT lines were included, and the spectrum obtained this way is still an approximate one. An exact spectrum can be calculated by including all the SQT lines in Fig 4.6b. For simplicity, here we use a three-spin system to explain this difference. Also, during the Jacobi transformation, high-order cross terms (corresponding to couplings of 4, 6, ..., 2m spins) will be created, which will lead to new off-diagonal elements being created. If their values become too large, they also must be eliminated.

§ 4.2.3 Speed Advantage

From the calculation of N(SQT) in §3.4, we obtained

$$N(SQT) = \Sigma_k C^k{}_N C^{k+1}{}_{N-k} 2^{N-2k-1} + C^1{}_N 2^{N-1} \qquad [4.7]$$

and we know

$$N(SSSQT) = N2^{N-1}. \qquad [4.8]$$

So the ratio ζ = N(SQT)/N(SSSQT) as a function of N can be estimated through a calculation for N = 2 to 20 (Fig 4.7).

From Fig 4.7 it can be seen that a factor ~10^6 for compression in the computing load will be available for an N=20 spin system, if SSSQT are taken as an approximate spectrum. When N=17, this factor is about ~10^3, making it possible to get the spectrum within 19.5 cpu hours on a microvax-II machine.

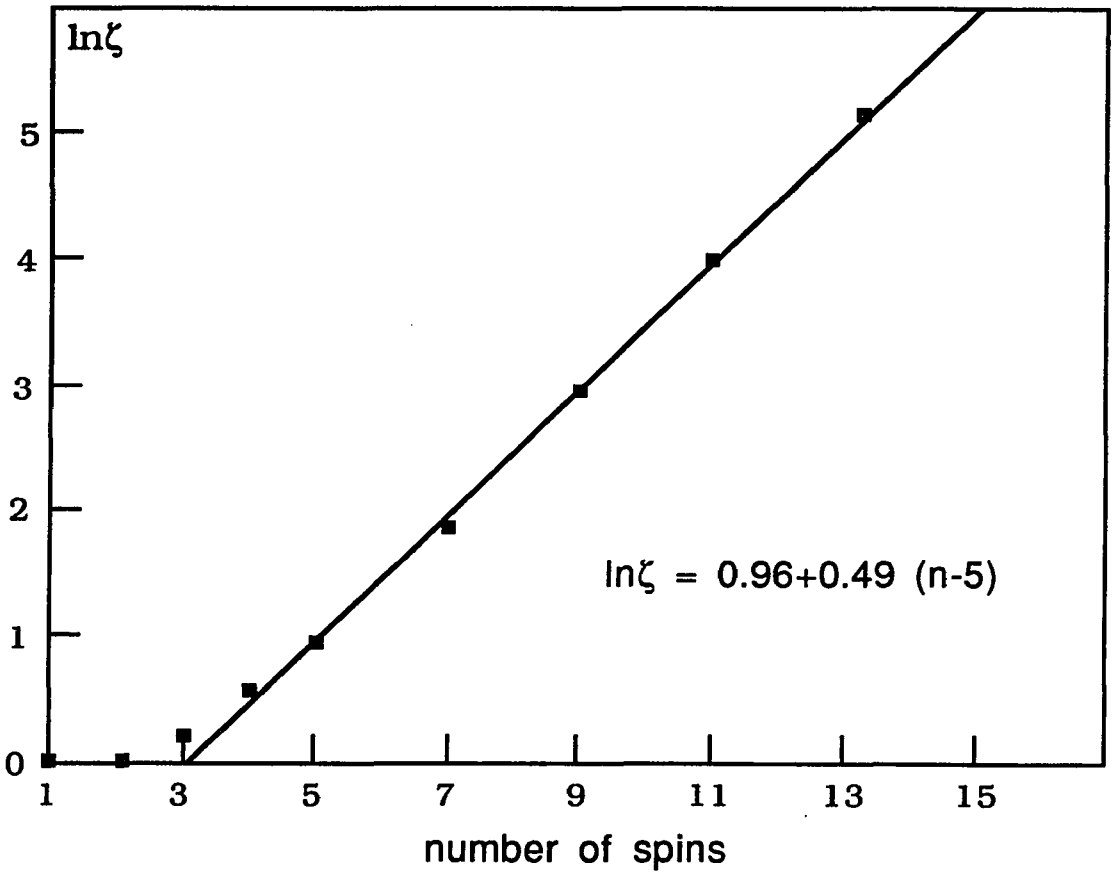

Fig 4.7 The ratio ζ = N(SQT)/N(SSSQT) as a function of N. When N>5, ζ increases exponentially with a slope of ~0.49.

Section 5 Outline of SIMPL

§ 5.1 Logical Structure

There are three modes of operation: 1D SQT, 1D SSSQT, and 3D SSSQT. The first two modes use the recursive formula expressed in Fig 4.5 and 4.6 to diagonalize the Hamiltonian matrix and to transform σ, F^+ matrices. The third mode first uses a simple data base to store the approximate chemical shift values of the Hydrogen-1, Carbon-13 and Nitrogen-15 nuclei of the twenty aminoacids. The first step in this mode is to create an approximate 3D data set. Then, the experimental 3D data set is displayed together with the simulated one, but in different color. With the help of the three 2D section planes (XY, YZ, and XZ sections) of the 3D spectrum, these three 2D spectra are simultaneously displayed, which can be used to compare with the characteristic cross peak patterns of the 20 amino acids. As the thickness of the section planes are adjustable, and the sequence of the residues are known, the user can pick up any one residue, and display it separately. Another convenience is that the user can display (in different colors) the inter-residue NOE

peaks (obtained from NOESY experiments) between the α-proton and NH-proton, even for a COSY-COSY spectrum. These inter-residue NOE peaks are used to direct the 'navigation' of the cursor in the 3D spectral 'space'. If one residue of the peptide can be recognized and its peaks are assigned, then the user can move the simulated peaks to coincide with the assigned experimental peaks. Since when any one coordinate of any one peak is changed, all the cross peaks between this peak and other peaks will change, all these cross peaks will be moving together. With the help of the inter-residue NOE peaks, the next residue will be 'pulled out', and by comparing the cross peak pattern, the spectral lines of the next residue will be recognized. The idea is the same as the manual assignment, but the simultaneous display of the NOE peaks in the COSY-COSY spectrum, and the simultaneous display of the ^{1}H-^{1}H and ^{13}C-^{1}H cross COSY spectra provide extra convenience for the assignment. As all the experimental peaks coincide with the simulated peaks, the assignment is completed. After this, the third step is to interface the simulation program with the molecular modeling program, and display the approximate NOE peaks using the nuclear coordinate information provided by the modeling program.

§ 5.2 Flowchart and graphics program structure

Fig 5.1 is a flowchart of SIMPL(1D) module. Fig 5.2 is a flowchart of SIMPL(3D) module. Fig 5.3a - 5.3d are the data structure of the graphics program of SIMPL. All of these are written in VAX FORTRAN and VAX/VMS graphical support routines (GSR) of the E & S PS-390 graphics package JCP A3V03[17].

§ 5.3 Simulation Examples

Fig 5.4 shows one simulation example made by SIMPL. Fig 5.5 shows the convergence performance of SIMPL(1D); it took ~13.5 cpu hours to diagonalize the Hamiltonian matrix of a 14-spin coupling network. The largest off-diagonal element is monotonically decreased by the Jacobi transformations.

Fig 5.6 is a comparison between SIMPL(1D) and a Jacobi diagonalization program, on the same computer, under the same operating environment. The largest coupling network that can be calculated by the Jacobi method is only a six-spin system. Although both programs have not been optimized, and the measurement of

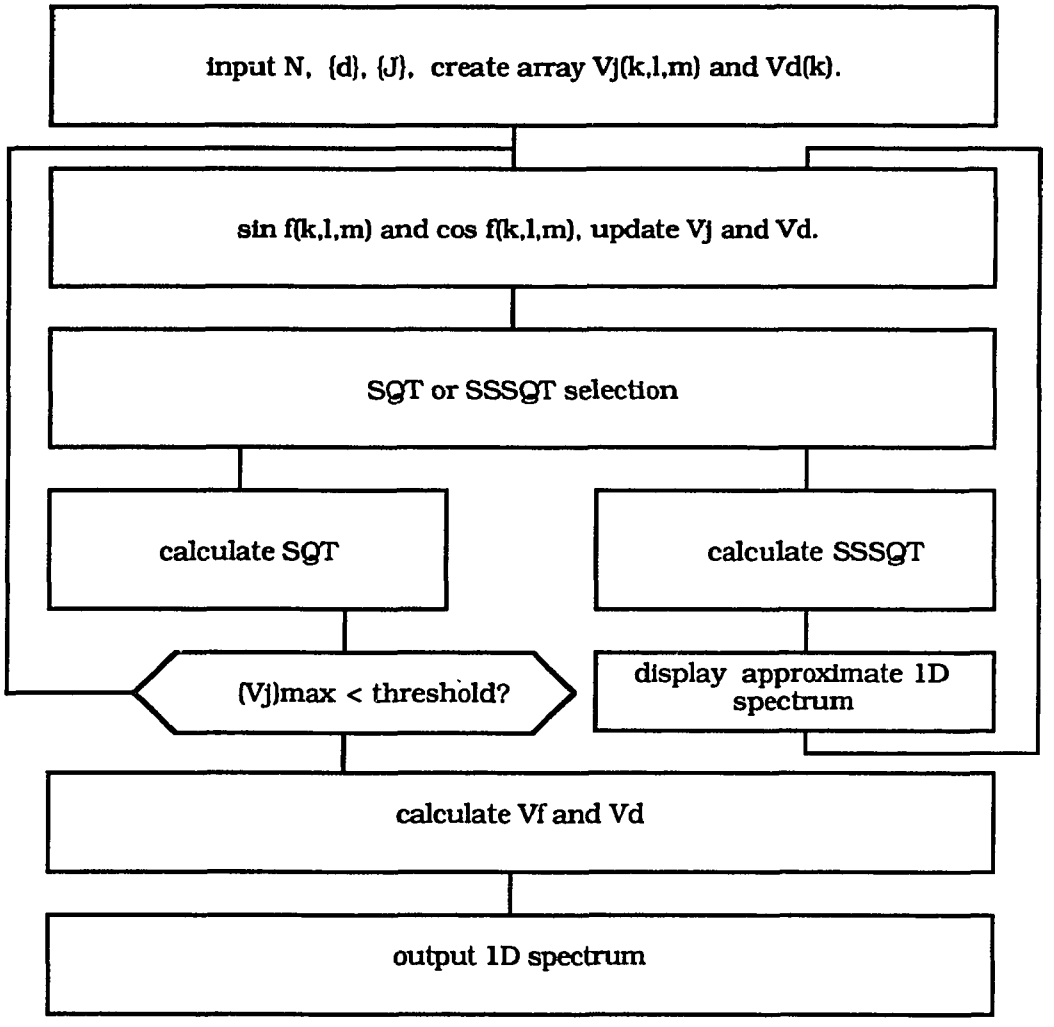

Fig 5.1 Flowchart of SIMPL (1D).

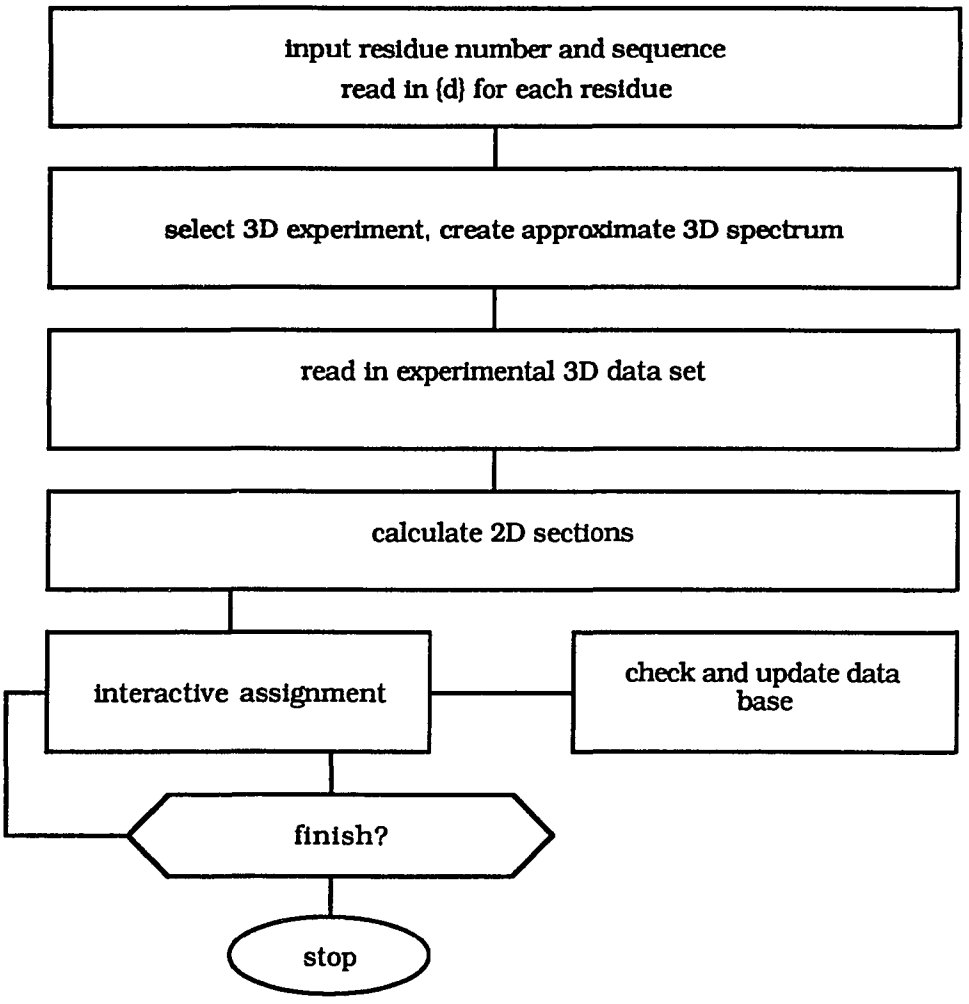

Fig 5.2 Flowchart of SIMPL (3D).

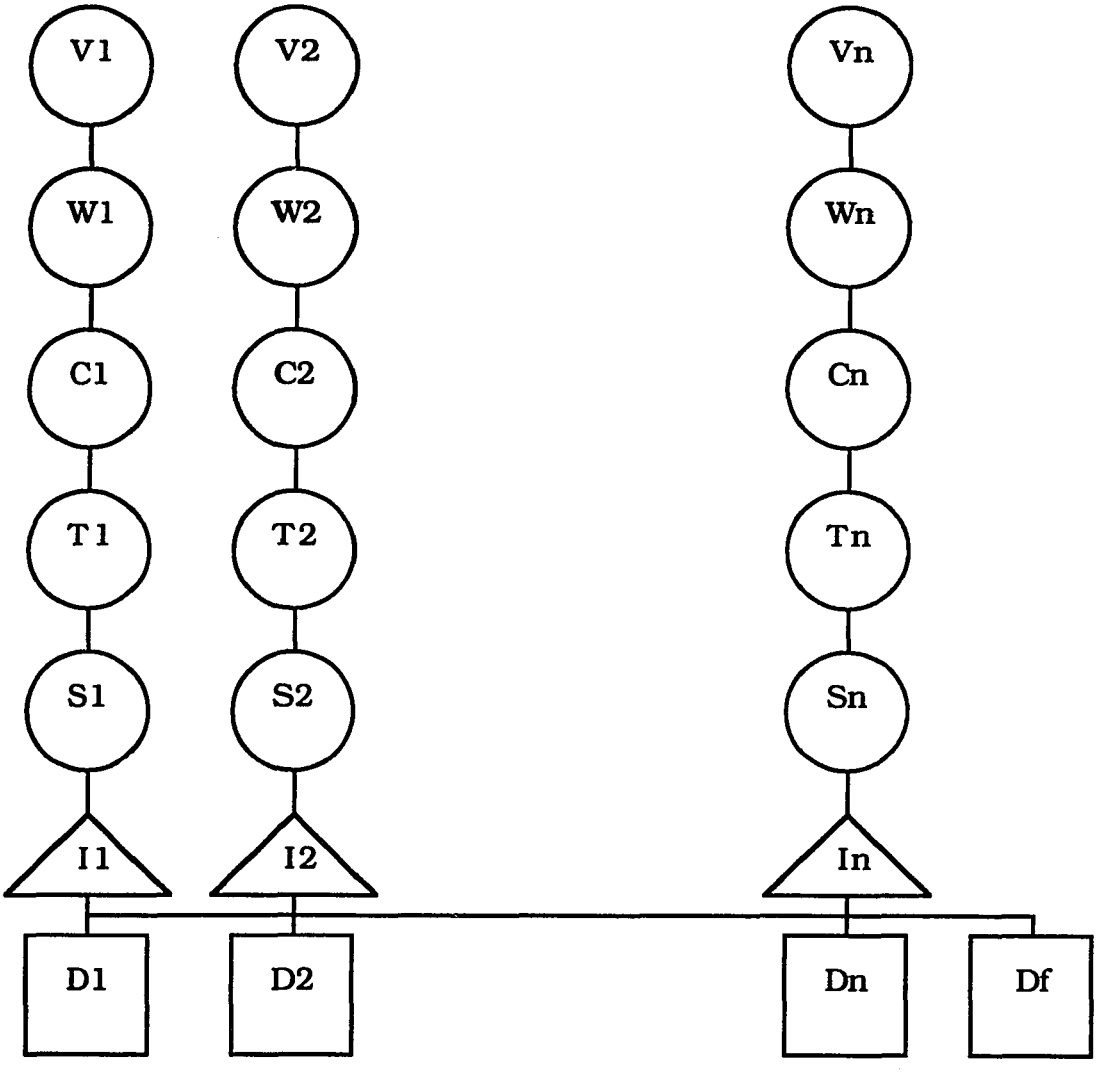

Fig 5.3a Graphics data structure of SIMPL, Pt1 V-viewport, W- window, C-color, T-translate, S-scale, I-instance, D-data

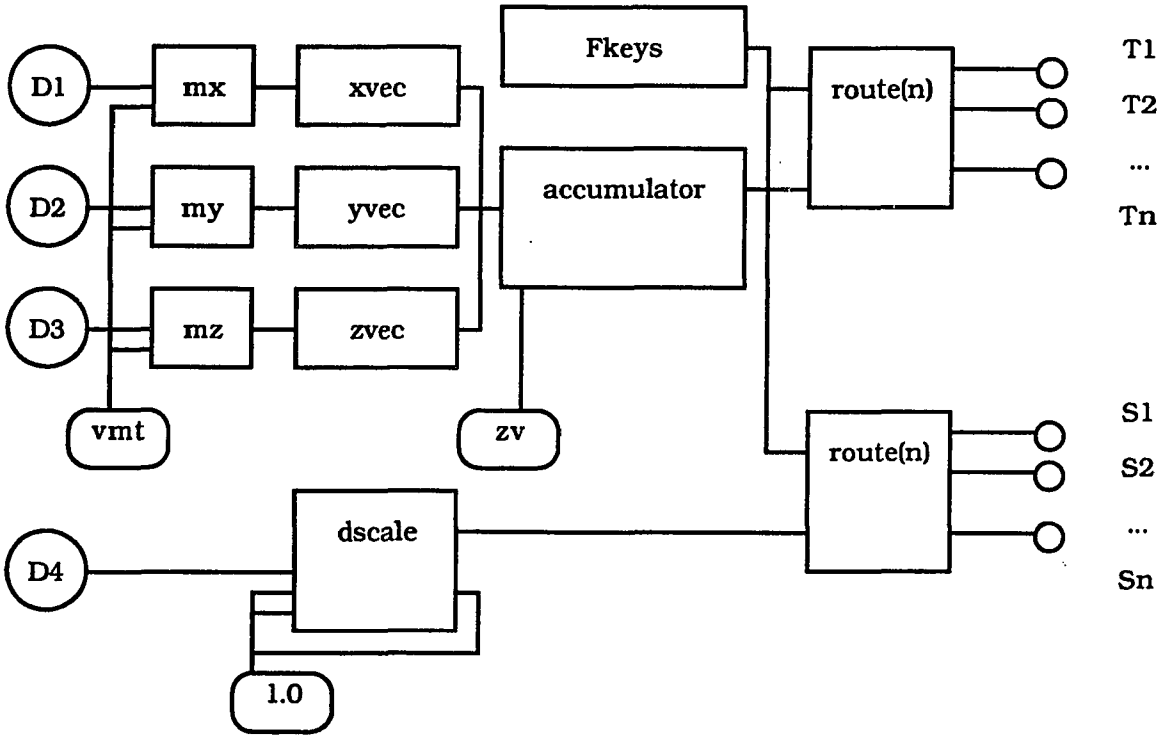

Fig 5.3b Graphics data structure of SIMPL, Pt2

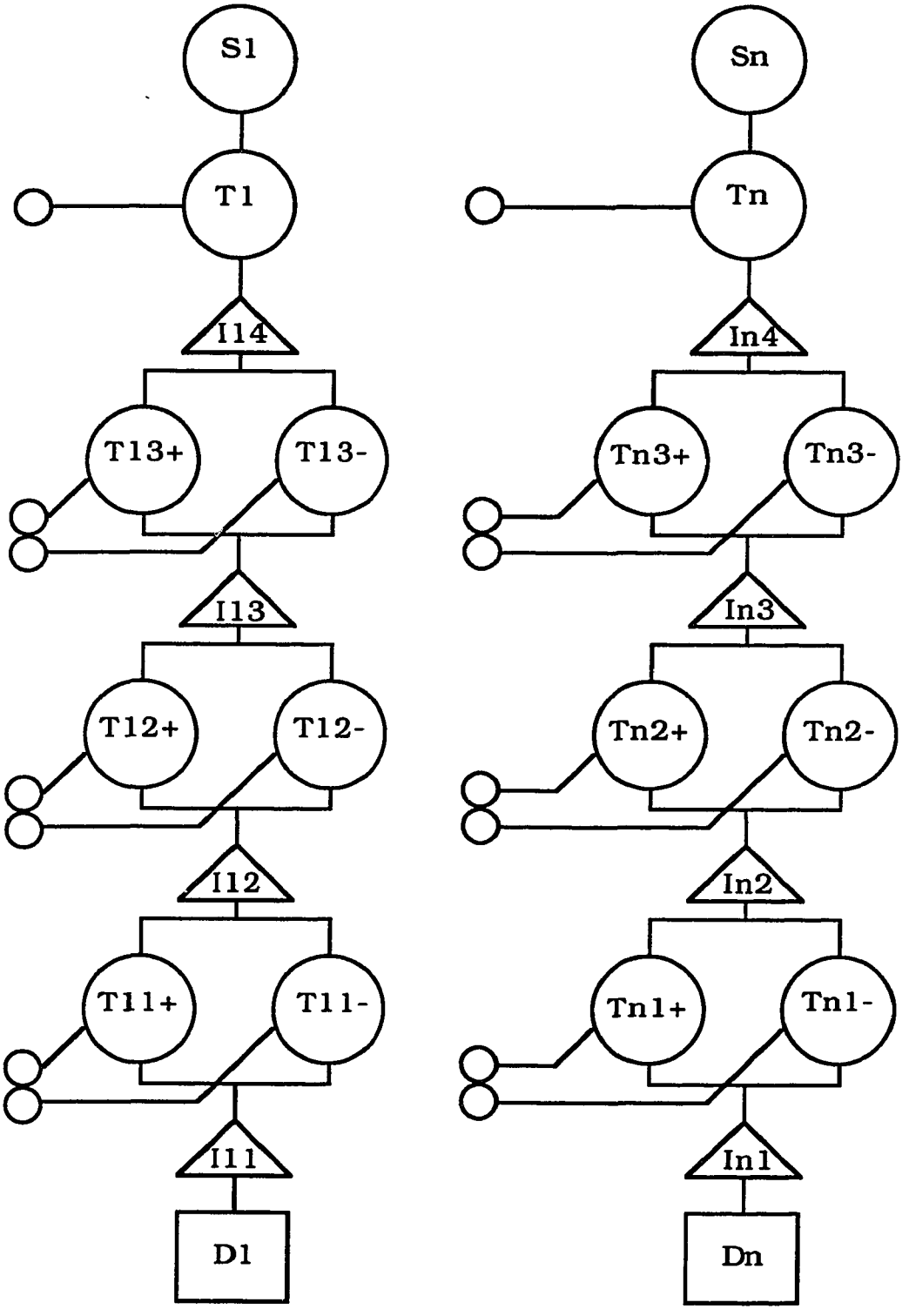

Fig 5.3c Graphics data structure of SSSQT simulation module, data transformation part. D - data, T - translation, I - instance, S - scale.

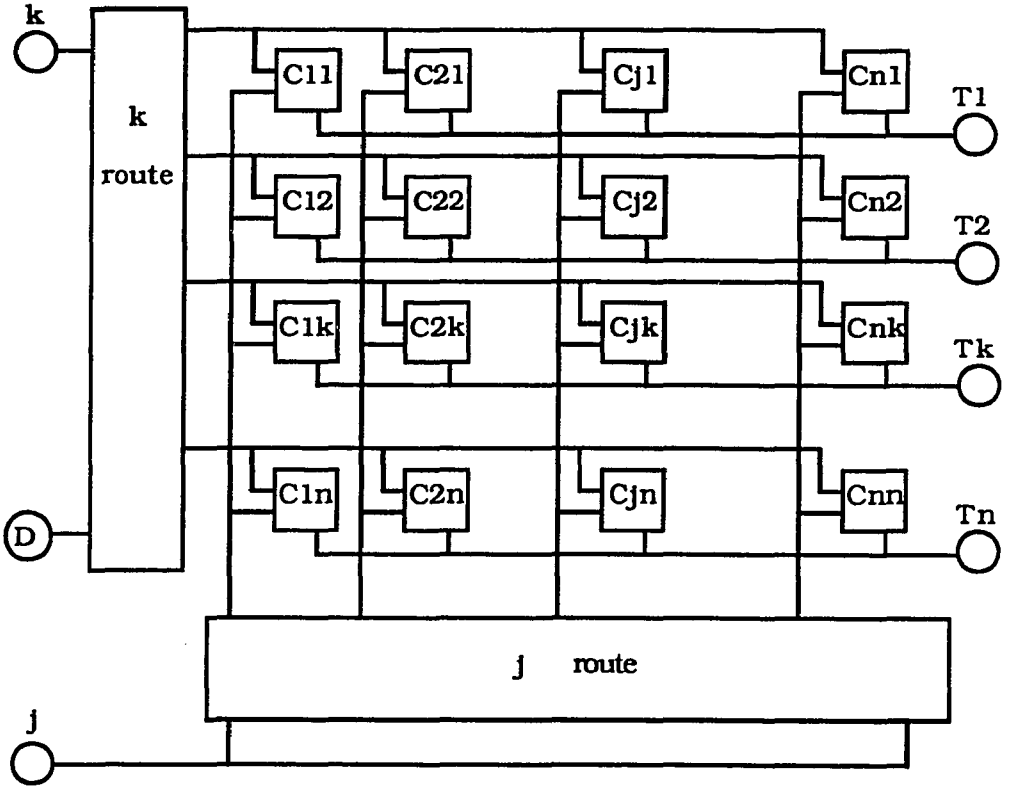

Fig 5.3d Graphics data structure of SSSQT simulation module, control network part. Cjk - constant function instances.

G'GXS

β-D-Galp-(1→3)-β-D-Galp-(1→4)-β-D-Xylp-(1→O)-L-Ser

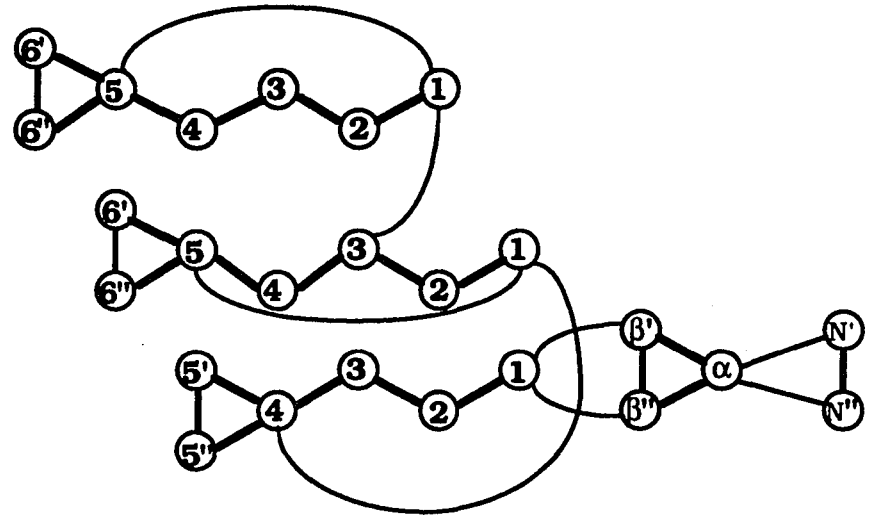

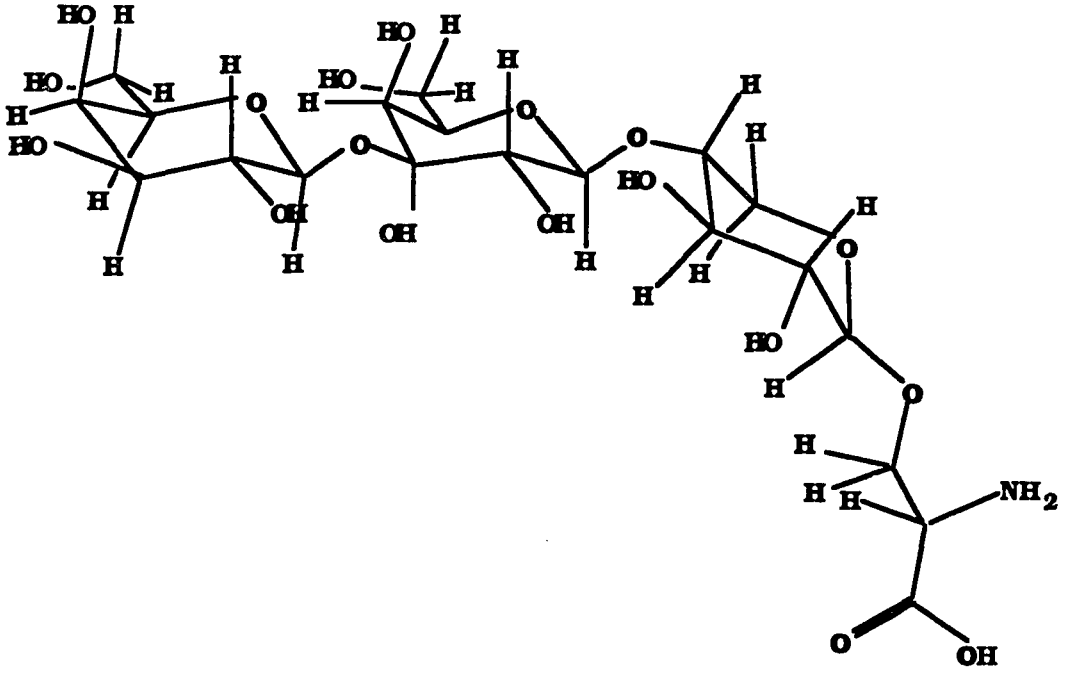

Fig 5.4a An example of 1D spectrum simulation (see ref. [24]).

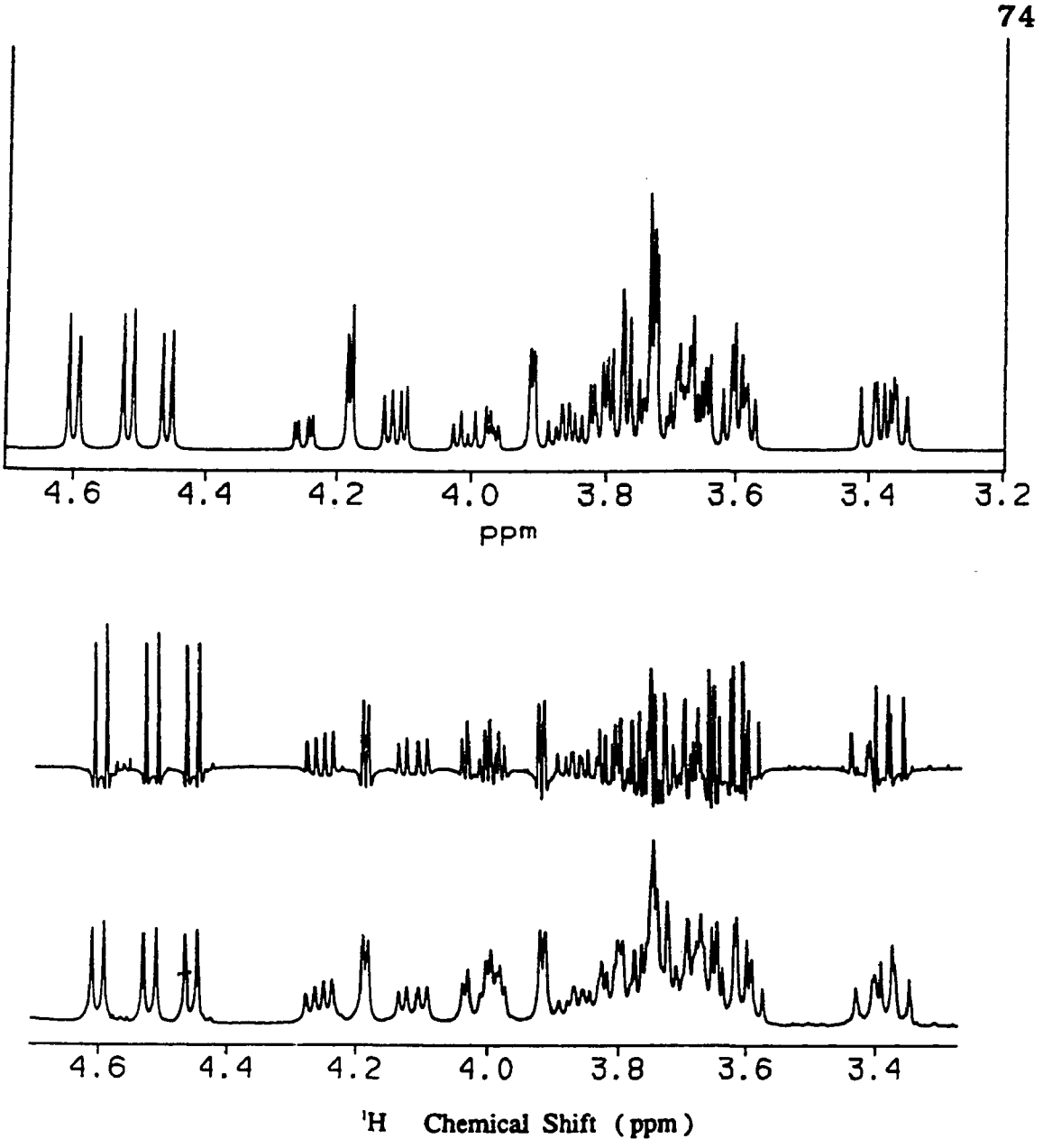

Fig 5.4b The 1D experimental and simulated spectra of G'GXS. top: simulated spectrum by SIMPL; middle: resolution enhanced (by maximum entropy method) experimental spectrum; bottom: experimental spectrum.

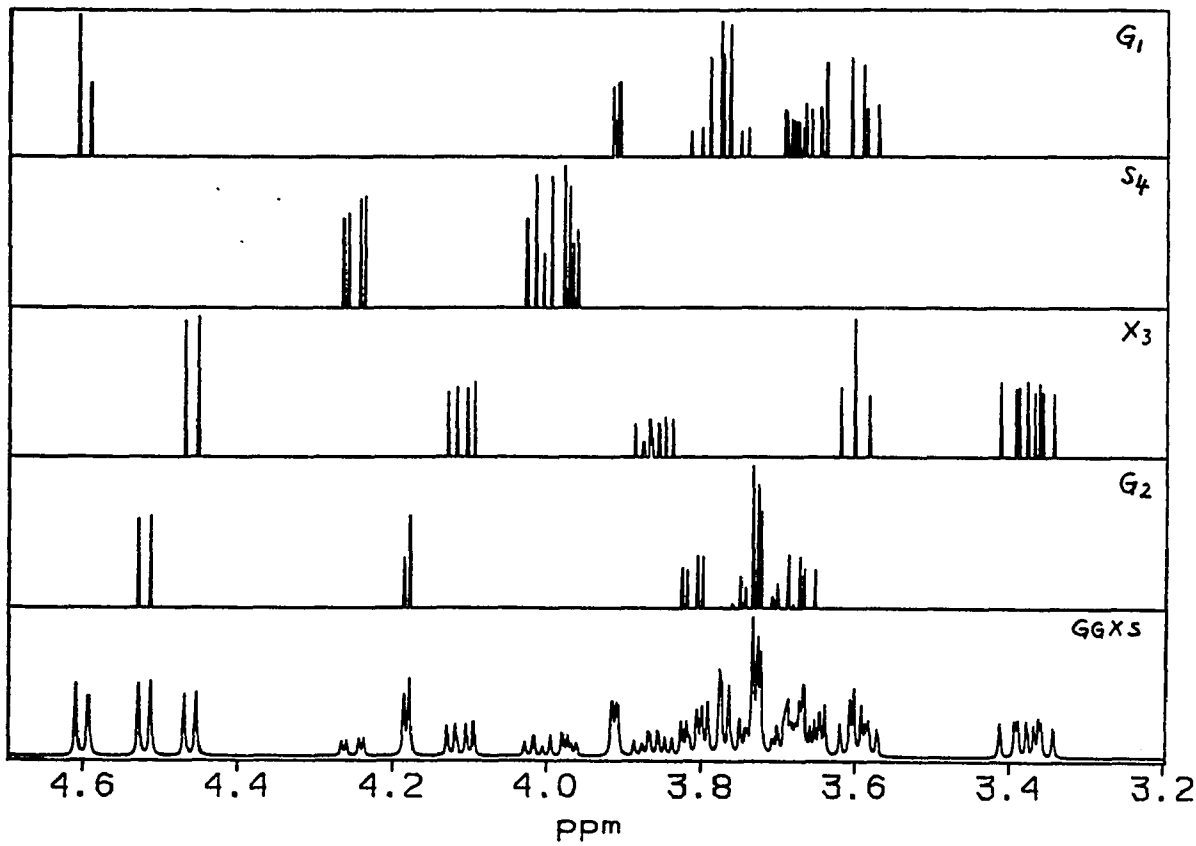

Fig 5.4c The separately simulated results of four coupling networks of G'GXS, and the summation of all four parts (bottom).

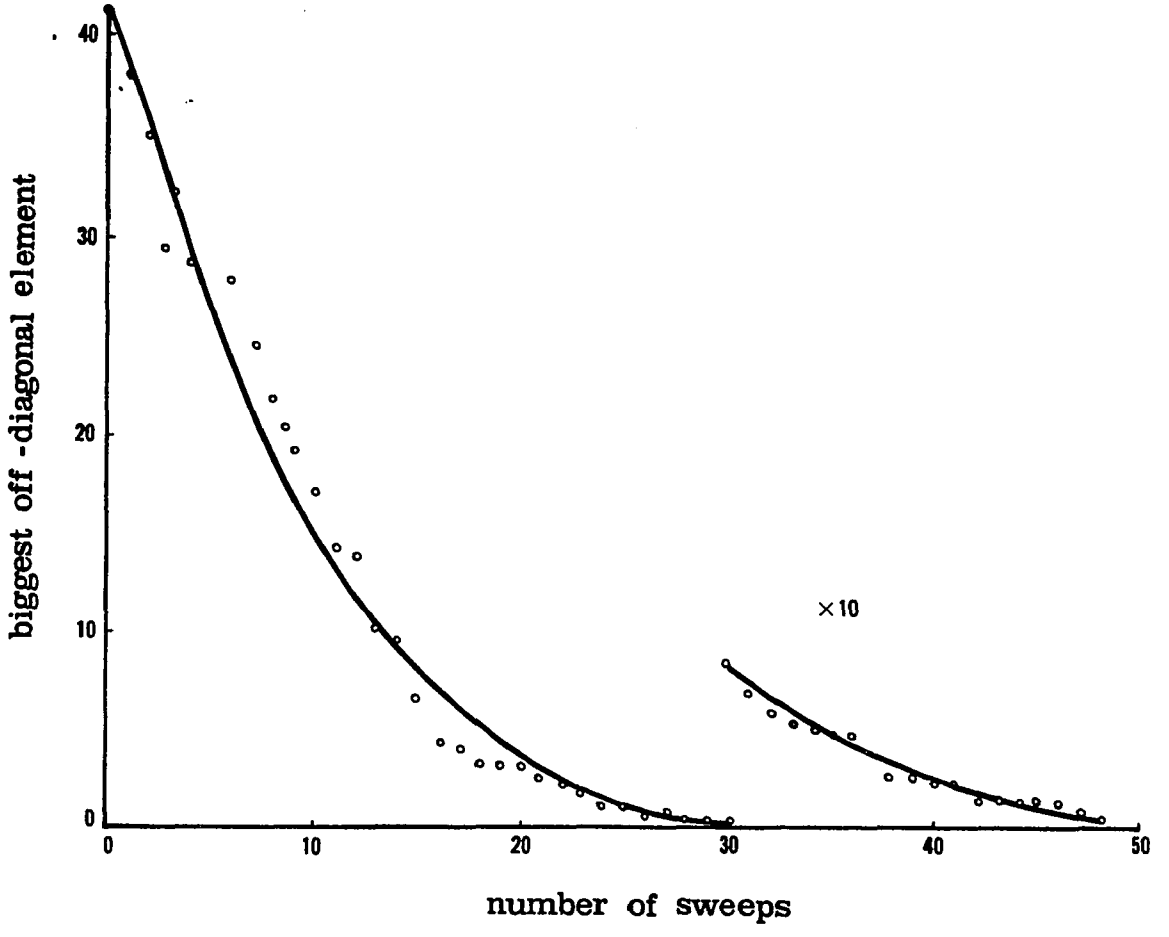

Fig 5.5 The convergence performance of SIMPL. The Hamiltonian matrix of a fourteen-spin coupling network has been diagonalized after 48 iterations of Jacobi rotations. This is equivalent to 4096 Jacobi rotations on this 16384^2 matrix in each iteration, if it is done by the Jacobi method.

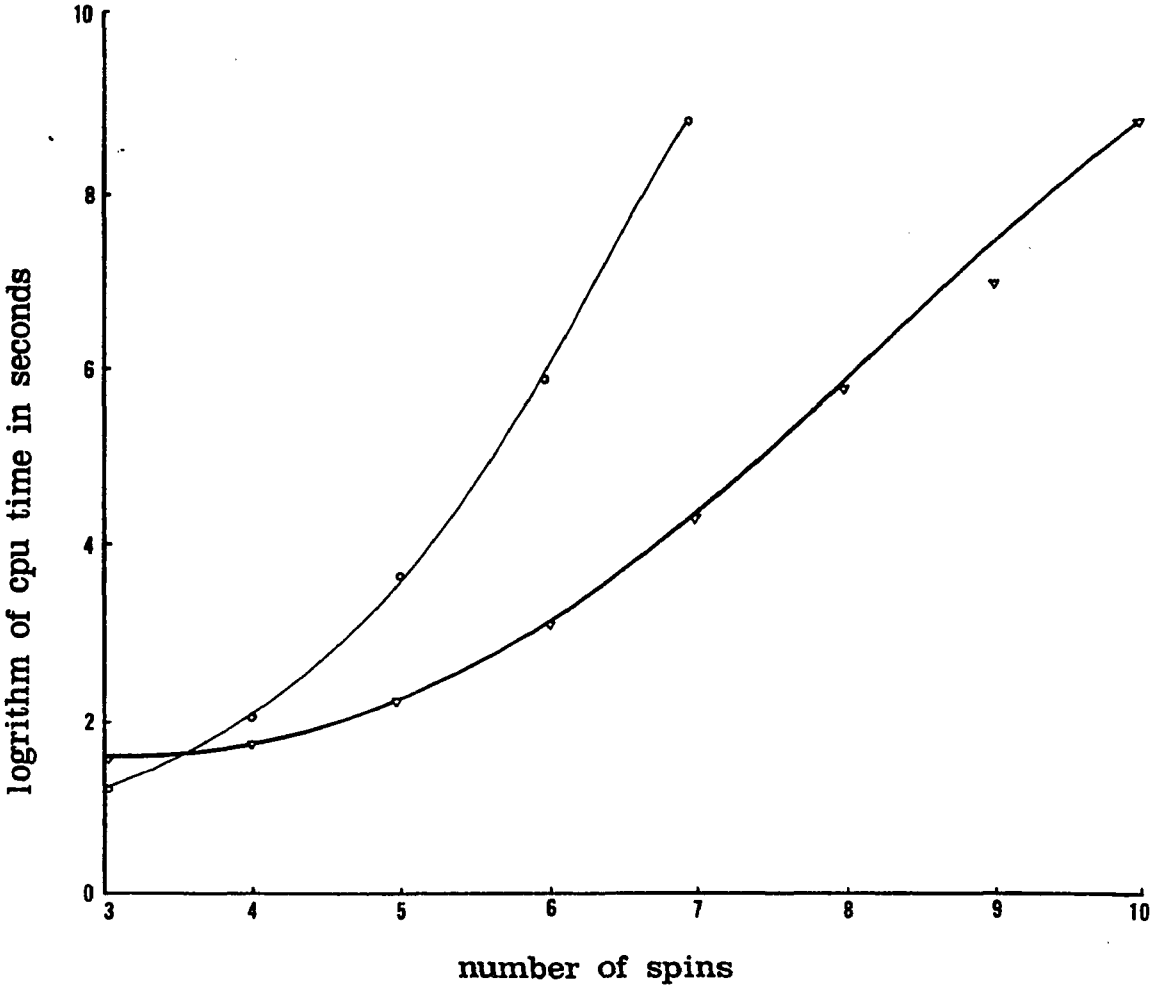

Fig 5.6 A comparison between SIMPL and a Jacobi diagonalization program on a microvax-II computer with 9MB board memory.

the running time includes the data input overhead processing time, which varies from time to time under the ordinary multi-user, multi-task operating environment, still the relative relation between the running time and the spin numbers coincides with the estimation of the computing load of the two methods.

§ 5.4 Interactive Assignment

Fig 5.7 is an example of using SIMPL(3D) as an interactive assignment tool. From the published data of Interluekin-1β by Driscoll and Clore et al[19,20], an approximate 3D spectrum of this 153-residue peptide was created. The ^{1}H, ^{13}C and ^{15}N chemical shift data were randomly picked up from a simple data base, which also is made of the data in references[3, 20]. The size of the 3D peaks were displayed as the average line width of the three dimensions of F_1, F_2, and F_3, and a 17~61 points ovalsphere line shape function was assumed for all the peaks. For the three section planes moving along X, Y, and Z axes, a thickness of 10 times the linewidth along their moving axis was selected, and only those peaks within these planes were displayed.

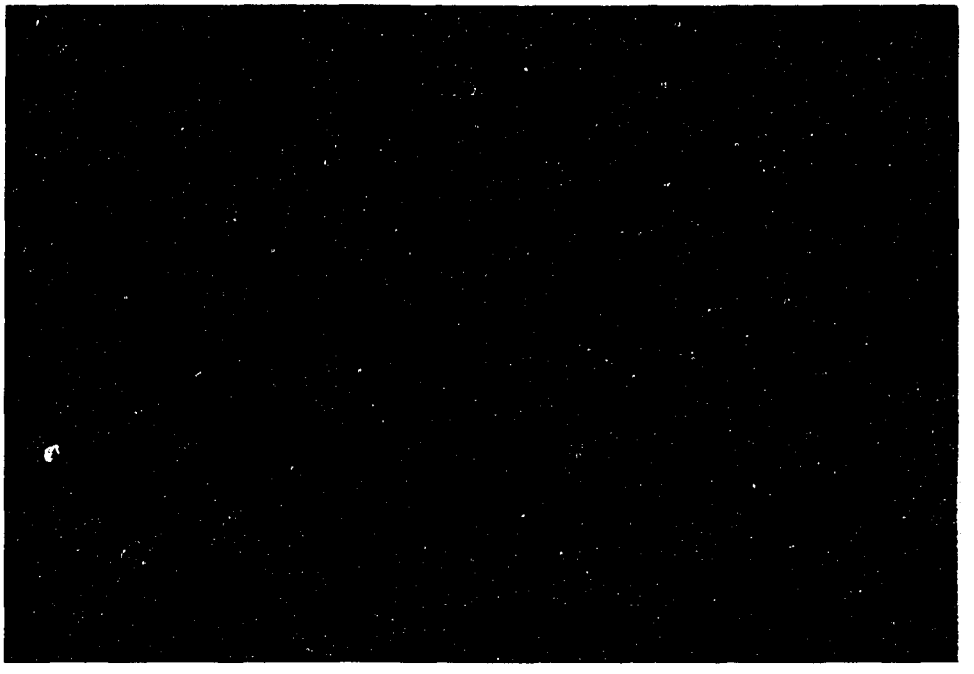

Fig 5.7 Interactive assignment by SIMPL (3D) on E&S PS390 system. The 3D COSY-COSY spectrum is displayed at the upper left corner. Three 2D sections at upper right, lower left, and lower right corners are X, Y, and Z sections, respectively. X, Z or F_1, F_3 are ^1H frequency axes; Y or F_2 is ^{13}C frequency axis.

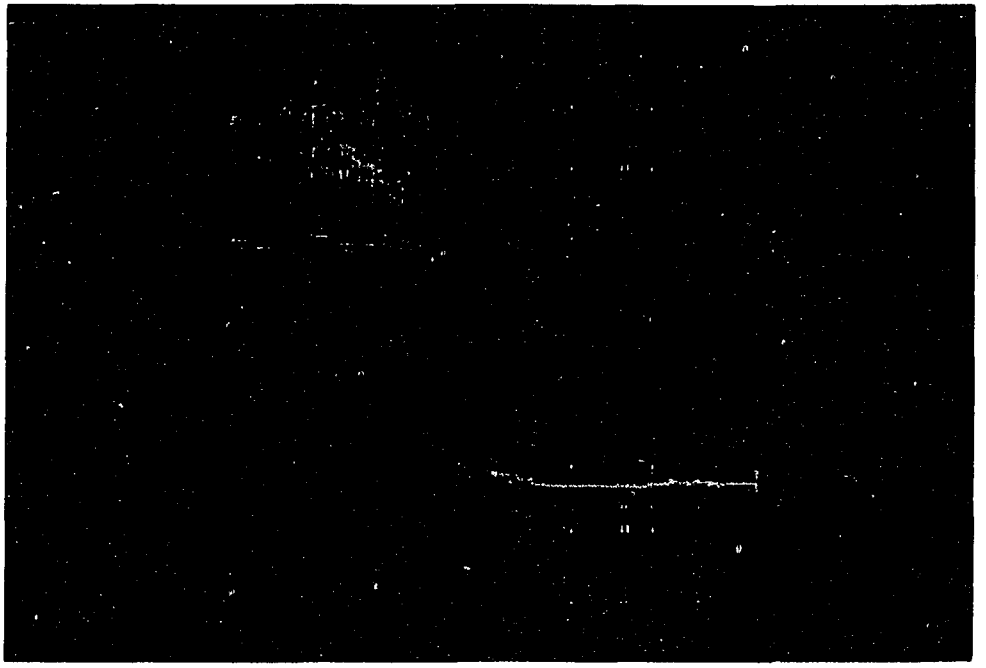

Fig 5.7 (Cont.) The same spectrum as on the previous page, but as the cursor moves, the three 2D section planes are moving simultaneously, showing the different 2D slices of the 3D data set.

Compared with the experimental data, however, these are equivalent to a much better digital resolution in at least one of the three dimensions. Since no experimental data other than that previously published was available, this comparison is only a symbolic one. With such a premature simulation, the only purpose is to show the practicality and convenience of the 3D simulation by SIMPL. It not only provides a tool for interactive assignment, but much more importantly, it provides an interface between a 3D spectrum and the molecular modeling program as well. With a modeling program to manipulate the coordinates of the atoms, through this interface one can see the real-time changes of the 3D spectrum.

Summary

As nmr spectroscopy is becoming more and more important to the research of molecular structure (especially in the solution environment), there grows a demand for an efficient approach to predict nmr spectra of several candidate structures of an unknown molecule, or of several different conformations of a biological polymer with known primary structure, and for interactive comparison with experimental spectra. This work is targeted to this purpose. By a novel rearrangement of the state functions of a spin system into a special sequence, the system's Hamiltonian matrix will appear in a highly symmetrical pattern, in which all the non-zero elements reside at positions which are precisely predictable throughout the entire process of matrix diagonalization. Therefore, the diagonalization can be done by updating the values of all these elements according to a group of recursive formulae. Since the matrix transformation and multiplication are replaced by one dimensional array processing, much larger systems can be handled compared with the ordinary method. Furthermore, according to a

quantitative analysis of the error introduced by ignoring the observable combined lines in the 1D spectrum, situations have been recognized in which the entire spectrum can be safely approximated by Single Spin Single Quantum Transitions (SSSQT) for most practical applications. This approximation dramatically saves computing time, and the saving will increase exponentially with the number of spins in the system, and makes possible interactive modification of chemical shift and J coupling constant values within seconds, thus realizing "real-time" nmr spectrum simulation.

Combined with the SSSQT approximation and a simple data base made from published chemical shift data of peptides, an estimated 3D nmr spectrum for peptide of less than 200 residues can be created and displayed together with experimental ones. This not only provides 'hints' for the manual assignment process, but more importantly, it can be used as an interface between a molecular modeling program and an experimental nmr spectrum. While the user is manipulating a molecular model on the graphics screen, the 3D simulated spectrum, together with its 2D or 1D section slides, can be monitored continuously, realizing an interactive comparison directly between a changing conformation and an nmr spectrum.

Appendix: NMR Signal Function S(t)[5]

A 1D nmr spectrum is an intensity function of frequency, $I(\omega)$. It is the Fourier transformation of a signal function of time, S(t):

$$I(\omega) = FT \{ S(t) \} \qquad [1]$$

This signal function is the time-dependent voltage acquired by the probe coil around the sample at the detecting moment, t.

According to Faraday's law, this signal voltage equals the time derivative of the magnetic flux through the effective surface A of the probe coil:

$$S(t) = dF/dt = d/dt \int_A B(t)\, da = \int_A d/dt\, B(t)\, da \qquad [2]$$

where B(t) is the magnetic field created by the sample, and is proportional to the magnetization of the sample at the moment of t, providing the sample has the property that B(t) // M(t).

Usually the probe coil is designed such that its effective surface is perpendicular to the external magnetic field B_0, so if the

direction of B_0 is taken as the Z axis, the effective surface of the coil defines the XY plane.

Since the magnetization M(t) is experiencing a torque in the field B_0:

$$dM(t)/dt = M(t) \times \gamma B_0 \qquad [3]$$

and combine [2,3], one gets

$$S(t) \propto \int_A [M(t) \times \gamma B_o] \, da. \qquad [4]$$

Taking into account the fact that only the XY component of $[M(t) \times \gamma B_0]$ contributed to S(t),

$$S(t) \propto \gamma B_0 \int_A M_{xy}(t) da. \qquad [5]$$

For a given machine and probe, A and B_0 are constants, so

$$S(t) \propto M_{xy}(t). \qquad [6]$$

As a physically measurable quantity, $M_{xy}(t)$ can be described quantum mechanically:

$$< M_{xy}(t) > = Tr \{ \Sigma_k (I_x + iI_y)_k \sigma(t) \} \qquad [7]$$

where the summation runs over all spins (with subscript k for each), and I_{xk} and I_{yk} are the X and Y components of the nuclear spin

angular momentum of spin k, respectively; $\sigma(t)$ is the density matrix of the spin system at the moment of t.

References

1. Clore, G. M. and Gronenborn, A. M. (1991), Two-, Three-, and Four-Dimensional NMR Methods for Obtaining Large and More Precise Three-Dimensional Structures of Proteins in Solution, in *Annu. Rev. Biophys. Biophys. Chem.*, Vol. **20**, pp. 29-63; ed. by Engelman, D. M., Cantor, C. R., and Pollard, T. D., Annual Review Inc. Palo Alto, California.

2. Ernst, R. R., Bodenhausen, G., and Wokaun, A. (1986), *Principles of Nuclear Magnetic Resonances in One and Two Dimensions*, Oxford University Press. Oxford.

3. Wuthrich, K. (1986), *NMR of Proteins and Nucleic Acids*, John Wiley & Sons, Inc. New York.

4. Pretsch, E., Furst, A., and Robien, W. (1991), *Analytical Chim. Acta* **248**, 415-428.

5 Abragam, A. (1961), *The Principles of Nuclear Magnetism*, Oxford University Press. Oxford.

6. Cohen-Tannoudji, C., Diu, B., and Laloe, F. (1987), *Quantum Mechanics*, Hermann, Paris.

7. Slichter, C. P. (1978,1980), *Principles of Magnetic Resonance*, Springer-Verlag. New York.

8. Van de Ven, F. J. M., and Hibers, C. W. (1983), *J. Magn. Reson.*, **54**, 512-520

9. Brown, W. R., and Bierer, J. (1983), *J. Magn. Reson.*, **68**, 217-231.

10. Blechta, V., and Schraml, J. (1986), *J. Magn. Reson.*, **69**, 293-301.

11. Nakashima, T. T., and McClung, R. E. D. (1986), *J. Magn. Reson.*, **70**, 187-203.

12. Hawarth, M. A., Lian, A. Y., Hawkes, G. E., and Sales, K. D. (1986), *J. Magn. Reson.*, **68**, 433-452.

13. Packer, K. J., and Wright, K. M. (1983), *Mol. Phys.*, **50**, 797-813.

14. Sorenson, O. W., Eich, G. W., Levitt, M. H., Bodenhausen, G., and Ernst, R. R. (1983), Product Operator Formalism for the Description of NMR Pulse Experiments, *Progr. Nucl. Magn. Reson. Spectros.*, **16**, 163-192.

15. Wilkinson, J. H., and Reinsch, C. (1971), *Handbook for Automatic Computation*, Vol **2**, Linear Algebra, Springer-Verlag, New York.

16. Smith, B. T. et al. (1976), Matrix Eigensystem Routines - EISPACK Guide, 2nd. ed., Vol **6** of *Lecture Notes in Computer Science*, Springer-Verlag, New York.

17. Poole, C. P. and Farach, H. (1976, 1987), *Theory of Magnetic Resonance*, John Wiley & Sons, Inc. New York.

18. Swalen, J. D. (1966), Computer Techniques in the Analysis of NMR Spectra, *Progr. Nucl. Magn. Reson. Spect.*, **1**, 205-250.

19. Schaublin, S., Hohener, A., and Ernst, R. R. (1974), *J. Magn. Reson.*, **13**, 196-216.

20. Widmer, H. and Wuthrich, K. (1986), *J. Magn. Reson.* **70**, 270-279.

21. Celda, B., Widmer, H., Leupin, W., Chazin, W. J., Denny, W. A., and Wuthrich K. (1989), *Biochemistry*, **28**, 1462-1471.

22. Zhou, N., Manogaran, S., Zon, G., and James, T. L. (1988), *Biochemistry*, **27**, 6013-6020.

23. PS390 Document Set, Evans & Sutherland Computer Corporation (1987), Salt Lake City, Utah.

24. Choe, B., Ekborg, G., Roden, L., Harvey, S. C., and Krishna, N. R. (1989), NMR and Modeling Studies on Carbohydrate-Protein Linkage Region Fragments from Connective Tissue Proteoglycans, in *Sixth Conversation in Biomolecular Stereodynamics*, pp. 52, ed. by Sarma, R. H., Institute of Biomolecular Stereodynamics, SUNY at Albany, New York.

25. Driscoll, P. C., Clore, M., Marion, D., Wingfield, P. T., and Gronenborn, A. M. (1990), *Biochemistry*, **29**, 3542-3556.

26. Clore, G. M., Bax, A., Driscoll, P. C., Wingfield, P. T., and Gronenborn, A. M. (1990), *Biochemistry*, **29**, 8172-8184.

27. Groβ, K. H., and Kalbitzer, H. R. (1988), *J. Magn. Reson.*, **76**, 87-99.